FEATURE ARTICLE

The $C_2H_5 + O_2$ Reaction Mechanism: High-Level ab Initio Characterizations

Jonathan C. Rienstra-Kiracofe,[†,‡] Wesley D. Allen, and Henry F. Schaefer III*

Center for Computational Quantum Chemistry, University of Georgia, Athens, Georgia 30602-2525

Received: March 17, 2000; In Final Form: June 13, 2000

The $C_2H_5^\bullet + O_2$ reaction, central to ethane oxidation and thus of fundamental importance to hydrocarbon combustion chemistry, has been examined in detail via highly sophisticated electronic structure methods. The geometries, energies, and harmonic vibrational frequencies of the reactants, transition states, intermediates, and products for the reaction of the ethyl radical ($\tilde{X}\ ^2A'$) with O_2 ($X\ ^3\Sigma_g^-$, a $^1\Delta_g$) have been investigated using the CCSD and CCSD(T) ab initio methods with basis sets ranging in quality from double-zeta plus polarization (DZP) to triple-zeta plus double polarization with f functions (TZ2Pf). Five mechanisms (M1−M5) involving the ground-state reactants are introduced within the context of previous experimental and theoretical studies. In this work, each mechanism is systematically explored, giving the following overall 0 K activation energies with respect to ground-state reactants, E_a(0 K), at our best level of theory: (M1) direct hydrogen abstraction from the ethyl radical by O_2 to give ethylene + $HO_2^\bullet$, E_a(0 K) = +15.1 kcal mol^{-1}; (M2) ethylperoxy β-hydrogen transfer with O−O bond rupture to yield oxirane + $^\bullet$OH, E_a(0 K) = +5.3 kcal mol^{-1}; (M3) ethylperoxy α-hydrogen transfer with O−O bond rupture to yield acetaldehyde + $^\bullet$OH, E_a(0 K) = +11.5 kcal mol^{-1}; (M4) ethylperoxy β-hydrogen transfer with C−O bond rupture to yield ethylene + $HO_2^\bullet$, E_a(0 K) = +5.3 kcal mol^{-1}, the C−O bond rupture barrier lying 1.2 kcal mol^{-1} above the O−O bond rupture barrier of M2; (M5) concerted elimination of $HO_2^\bullet$ from the ethylperoxy radical to give ethylene + $HO_2^\bullet$, E_a(0 K) = −0.9 kcal mol^{-1}. We show that M5 is energetically preferred and is also the only mechanism consistent with experimental observations of a negative temperature coefficient. The reverse reaction ($C_2H_4 + HO_2^\bullet \rightarrow {}^\bullet C_2H_4OOH$) has a zero-point-corrected barrier of 14.4 kcal mol^{-1}.

I. Introduction

The mechanisms of hydrocarbon combustion processes have fascinated chemists for more than 100 years.[1] In particular, the combustion of ethane (C_2H_6), being one of the simplest hydrocarbons and easily accessible experimentally, has drawn much attention.[2−7] Complete knowledge of the mechanism of ethane combustion has implications in a number of areas, such as atmospheric chemistry,[8−10] radical reaction chemistry,[11−20] fundamental studies of gas-phase ring intermediates,[21] and the development of transition state theories.[22,23] Proper understanding of ethane combustion establishes a prototype for combustion of higher alkanes. Yet, even today, many aspects of ethane combustion are surrounded by controversy and confusion. In this work we examine in detail some of the often nebulous mechanisms of ethane oxidation.

A. Early Mechanistic Theories of Hydrocarbon Combustion. Early hypotheses of ethane combustion arose from "hydroxylation theory",[24,25] which proposed alcoholic (hydroxylated) intermediates:

$$C_2H_6 + O_2 \rightarrow CH_3CH(OH)_2 \rightarrow CH_3CHO + H_2O \quad (1)$$

By the mid-1930s, however, hydroxylation theories had been more or less abandoned in favor of chain reaction mechanisms, as popularized by Semenov.[26] Chain reaction theories include the now familiar concepts of "initiation", "propagation", "branching", and "termination". Yet the mechanisms operative in each of these processes, for even a species as simple as ethane, were not understood. Indeed, in 1947, Cullis and Hinshelwood[27] remarked that "the experimental evidence on the subject of hydrocarbon oxidation is complex and the theoretical discussion confusing".

In their work, Cullis and Hinshelwood proposed that, in the presence of excess oxygen, alkane combustion proceeds through an initiation step in which radicals are produced through abstraction of a hydrogen atom by oxygen:

$$RH + O_2 \rightarrow R^\bullet + HO_2^\bullet \quad (2)$$

where $R^\bullet$ is an alkyl radical ($C_nH_{2n+1}^\bullet$) and RH the parent alkane. By the 1950s this initiation step and the importance of radical species in combustion was (and still is) generally accepted.[28] The radical species, $R^\bullet$, could then react with oxygen to form alkylperoxy radicals ($ROO^\bullet$)

$$R^\bullet + O_2 \rightarrow ROO^\bullet \quad (3)$$

* Corresponding author.
† E-mail: jrienst@emory.edu.
‡ Current address: Department of Chemistry, Emory University, Atlanta, GA 30322.

10.1021/jp001041k CCC: $19.00
Published on Web 10/13/2000

and specifically in the case of ethane

$$C_2H_6 + O_2 \rightarrow C_2H_5^{\bullet} + HO_2^{\bullet} \quad (4)$$

$$C_2H_5^{\bullet} + O_2 \rightarrow CH_3CH_2OO^{\bullet} \quad (5)$$

The fate of alkylperoxy radicals has been the subject of much debate. In 1954, Knox and Norrish[29] observed a "negative temperature coefficient" in the oxidation of ethane between 648 and 708 K. That is, the rate of oxidation decreases with increasing temperature over this range. This once-curious phenomenon was taken to represent a transition between the mechanisms operative at low temperatures and those at high temperatures. A number of different theories were put forth subsequently.

Although initial focus was on the isopropylperoxy and *n*-propylperoxy radicals, as well as higher alkylperoxy radicals, ethane combustion theory has its roots in these early hypotheses. Semenov[30] recognized the importance of alkylperoxy radical isomerization to hydroperoxyalkyl radicals, with decomposition of the latter:

$$C_nH_{2n+1}OO^{\bullet} \rightarrow {}^{\bullet}C_nH_{2n}OOH \quad (6)$$

$${}^{\bullet}C_nH_{2n}OOH \rightarrow C_nH_{2n} + HO_2^{\bullet} \quad (7)$$

Semenov thought that in the case of the isopropylperoxy and *n*-propylperoxy radicals, the barrier to isomerization (eq 6) would be about 20 kcal mol^{-1}. In contrast, Shtern[31] believed that the isopropylperoxy and *n*-propylperoxy radicals would decompose via initial scission of a carbon−carbon bond:

$$C_nH_{2n+1}OO^{\bullet} \rightarrow {}^{\bullet}R'-O-O-R'' \rightarrow R'{=}O + R''O^{\bullet} \quad (8)$$

Furthermore, experimental observations of ethylene as a product of ethane combustion led Lewis and von Elbe[32,33] to dismiss the alkylperoxy radical at higher temperatures in favor of direct bimolecular hydrogen abstraction by oxygen:

$$C_nH_{2n+1}^{\bullet} + O_2 \rightarrow C_nH_{2n} + HO_2^{\bullet} \quad (9)$$

According to Pollard,[33] for any mechanism to be correct, it must fulfill three requirements: "Firstly, it must be capable of explaining the mode of formation of the reaction products; secondly, it must be acceptable from thermokinetic considerations and finally, it must be capable of explaining phenomena such as the negative temperature coefficient . . ." Accepting the initiation step given in eq 2, the primary interest in this work is finding a quantitatively correct mechanism which, specifically in terms of the ethyl radical ($C_2H_5^{\bullet}$), satisfies these requirements.

B. Experimental Clues to the Nature of the $C_2H_5^{\bullet} + O_2$ Reaction. Most experimental work on the $C_2H_5^{\bullet} + O_2$ reaction observes at least one of ethylene (C_2H_4), oxirane (c-CH_2CH_2O), and acetaldehyde (CH_3CHO) as a primary product. All of these species have two carbon atoms, thus eliminating the decomposition mechanism of Shtern (eq 8). Therefore, we focus on five possible mechanisms, labeled as M1−M5 in the text, each leading to either ethylene, oxirane, or acetaldehyde as a product.

The first mechanism is the simplest (cf. eq 9):

(M1) direct hydrogen abstraction from the ethyl radical by O_2

$$C_2H_5^{\bullet} + O_2 \rightarrow C_2H_4 + HO_2^{\bullet}$$

The work of Knox and Wells[34−36] in the mid-1960s supported this bimolecular mechanism at temperatures between 598 and 698 K, and bimolecular abstraction was assumed in many subsequent studies.[37−41] Over the range of 698−838 K, Baldwin et al.[41] in 1980 suggested an activation energy of 3.9 kcal mol^{-1} for M1. Furthermore, Baldwin recognized the possibility of the other two products, oxirane and acetaldehyde, both of which are considerably more exothermic in terms of the overall reaction. The former was present in their experiments by a ratio of 1:100 compared to ethylene. In this case, they assumed a second mechanism, M2 (cf. eq 6)

(M2) ethylperoxy β-hydrogen transfer with O−O bond rupture

$$C_2H_5^{\bullet} + O_2 \rightarrow CH_3CH_2OO^{\bullet} \rightarrow {}^{\bullet}CH_2CH_2OOH \rightarrow c\text{-}CH_2CH_2O + {}^{\bullet}OH$$

and assigned a barrier of 34.3 ± 2.4 kcal mol^{-1} for β-hydrogen transfer relative to the ethylperoxy radical. Additionally, further evidence suggested that the formation of the most exothermic product, acetaldehyde, proceeded through an even larger barrier by an analogous, third mechanism, M3:

(M3) ethylperoxy α-hydrogen transfer with O−O bond rupture

$$C_2H_5^{\bullet} + O_2 \rightarrow CH_3CH_2OO^{\bullet} \rightarrow CH_3\dot{C}HOOH \rightarrow CH_3CHO + {}^{\bullet}OH$$

Earlier (1975), Hickel[42] suggested that, at least in solution, M1 was of little importance. Additionally, in examining the negative temperature coefficient of ethane, Dechaux and Delfosse[43] concluded in 1979 that the direct hydrogen abstraction route "is likely to be of negligible importance". (See also an earlier review by Fish.[44]) Instead Dechaux and Delfosse favored ethylperoxy radical isomerization (cf. eqs 6 and 7) according to a Semenov-type mechanism, M4:

(M4) ethylperoxy β-hydrogen transfer with C−O bond rupture

$$C_2H_5^{\bullet} + O_2 \rightarrow CH_3CH_2OO^{\bullet} \rightarrow {}^{\bullet}CH_2CH_2OOH \rightarrow C_2H_4 + HO_2^{\bullet}$$

In 1984, Slagle, Feng, and Gutman[45] studied the $C_2H_5^{\bullet} + O_2$ reaction over the temperature range of 294−1002 K. They found that the negative temperature coefficient extends to temperatures as high as 1000 K. The direct abstraction mechanism, M1, is inconsistent with this observation because the rates of elementary bimolecular reactions with positive activation energies, E_a, should increase with temperature. Instead, Slagle et al. argued that the highly exothermic equilibrium, $C_2H_5^{\bullet} + O_2 \rightleftharpoons CH_3CH_2OO^{\bullet}$, shifts to the left with increasing temperature, lowering the flux through the endothermic isomerization barrier for $CH_3CH_2OO^{\bullet} \rightarrow {}^{\bullet}CH_2CH_2OOH$. Assuming that this isomerization barrier and the barrier for ${}^{\bullet}CH_2CH_2OOH \rightarrow C_2H_4 + HO_2^{\bullet}$ decomposition are below reactants, M4 was taken to be consistent with the observed negative temperature coefficient. In support of this idea, Slagle et al. proposed that the ethylperoxy radical lies 29.5 kcal mol^{-1} (later revised[46] to 35.2 ± 1.5 kcal

mol^{-1} at 298 K) below reactants with a barrier for β-hydrogen isomerization of about 23 kcal mol^{-1}, which together yield an $E_a(0\ K) = -6.5$ kcal mol^{-1} for the entire $C_2H_5^\bullet + O_2$ reaction. A small barrier for the subsequent hydroperoxyethyl radical decomposition into products was also assumed (about 5−7 kcal mol^{-1} above products, which are about 13.0 kcal mol^{-1} below initial reactants).

In 1986 Baldwin, Dean, and Walker[47] studied the reverse reaction, $C_2H_4 + HO_2^\bullet \rightarrow {}^\bullet CH_2CH_2OOH$, and found an activation energy of 17.1 ± 1.2 kcal mol^{-1} (later revised[48] to 17.9 ± 1.1 kcal mol^{-1})—significantly more than the 5−7 kcal mol^{-1} suggested by Slagle et al.—which places the decomposition transition state above that of $C_2H_5^\bullet + O_2$, thus making M4 inconsistent with a negative temperature coefficient. Baldwin et al. further suggested that the barrier for $CH_3CH_2OO^\bullet \rightarrow {}^\bullet CH_2CH_2OOH$ is at least 31 kcal mol^{-1} and also above $C_2H_5^\bullet + O_2$. Additionally, they placed the barrier for decomposition of the hydroperoxyethyl radical to oxirane + $^\bullet$OH at only 16.5 kcal mol^{-1}, or 9.6 kcal mol^{-1} below that for decomposition to $C_2H_4 + HO_2^\bullet$. However, ethylene is the dominant product of the $C_2H_5^\bullet + O_2$ reaction, despite the greater exothermicity of the other possible products, oxirane and acetaldehyde. Thus, neither M2 nor M3 should be important. Believing then that M1−M4 were all inconsistent with experimental observations, Baldwin et al. proposed a new mechanism, M5, for ethylene formation:

(M5) concerted elimination of $HO_2^\bullet$ from the ethylperoxy radical

$$C_2H_5^\bullet + O_2 \rightarrow CH_3CH_2OO^\bullet \rightarrow C_2H_4 + HO_2^\bullet$$

In this mechanism, "concerted" does not imply that all ethylperoxy radicals are automatically converted to products, rather that no other genuine intermediate exists along the reaction path between the ethylperoxy radical and products. We note that Walker and co-workers[49,50] also argued against the mechanism favored by Slagle, Feng, and Gutman,[45] M4, but, concerned by the observation of Plumb and Ryan[51] that the overall reaction appeared to be independent of pressure (between 5 and 10 Torr of helium), argued in favor of a long-lived, cyclic $C_2H_5O_2^\bullet$ intermediate.

Subsequently, in a series of three studies (1989/1990), Wallington, Kaiser, and co-workers[52−55] demonstrated that contrary to the results of Plumb and Ryan, the overall rate of $C_2H_5^\bullet + O_2$ decreases after increasing pressure with various buffer gases, in agreement with earlier observations of Niki, Maker, Savage, and Breitenbach.[56] The ethylene yield fell from 12% $C_2H_5^\bullet$ consumption at 1 Torr to only 0.02% at 6000 Torr of air, indicating that a Lindemann-type mechanism is operative which stabilizes the ethylperoxy intermediate, as in every mechanism except M1, confirming that the ethylperoxy radical must be involved in the overall mechanism. These experimental observations, then, provided more evidence against the direct hydrogen abstraction process. Furthermore, in 1990, Bozzelli and Dean[57] used quantum Rice−Ramsperger−Kassel (QRRK) theory to model the kinetic data for the reverse reaction $C_2H_4 + HO_2^\bullet \rightarrow {}^\bullet CH_2CH_2OOH$ and obtained a barrier of only ≈8 kcal mol^{-1} for this reaction, as compared to the 17.1 kcal mol^{-1} originally proposed.[47] This revised barrier is below reactants; thus, if the β-hydrogen transfer barrier could also be found to be below reactants, there would be no need for ethylperoxy concerted elimination (M5).

Soon afterward (also 1990), Wagner, Slagle, Sarzynski, and Gutman[58] used Rice−Ramsperger−Kassel−Marcus (RRKM) theory fit to new experimental data to determine that the overall activation energy for $C_2H_5^\bullet + O_2 \rightarrow C_2H_4 + HO_2^\bullet$ was −2.4 kcal mol^{-1} at 0 K. Although Wagner et al. thought this barrier was that of the β-hydrogen isomerization transition state for $CH_2CH_2OO^\bullet \rightarrow {}^\bullet CH_2CH_2OOH$ in M4 (with the key assumption that $^\bullet CH_2CH_2OOH$ decomposition is also below reactants), their results could equally apply to that of ethylperoxy radical concerted elimination (M5).

Thus, by 1990, deductions from experiment had more or less ruled out the direct hydrogen abstraction (M1), and ethylene formation was believed to occur through isomerization of the ethylperoxy radical (M4), with neither oxirane nor acetaldehyde production playing a significant role (M2 and M3), presumably because of prohibitively high reaction barriers. Although concerted elimination of $HO_2^\bullet$ from the ethylperoxy radical (M5) had not been ruled out, nearly all subsequent experimental investigations[14,59−63] assumed M4, as favored by Wagner et al. Yet, in his 1992 review of the ethyl + O_2 reaction, Walker[64] clearly considered the evidence to date to as "controversial". Furthermore, in a 1995 review which also considered electronic structure data (discussed below), Pilling, Robertson, and Seakins[65] concluded that "the mechanism of Wagner et al. [M4] is incompatible with the significant lifetime of QOOH [hydroperoxyethyl radical] and its important position in alkane oxidation chemistry". Pilling et al. also drew upon theoretical work[66,67] to advocate a model which takes into account a second electronic surface involving the $C_2H_5^\bullet$ ($\tilde{X}\ ^2A'$) + O_2 ($a\ ^1\Delta_g$) reaction.

Finally, we highlight two important results from the most recent experiments: an upper limit on the overall activation energy for the $C_2H_5^\bullet + O_2 \rightarrow C_2H_4 + HO_2^\bullet$ reaction of +1.1 kcal mol^{-1} by Kaiser[63] and a new measurement of a −0.6 ± 0.1 kcal mol^{-1} activation energy by Dilger and co-workers.[61,62,68] We also note that Kaiser's[63] work concludes that the C_2H_4 yield at 298 K is less than 1%, but increases dramatically at temperatures above 400 K, confirming earlier, albeit limited, observations of Slagle and co-workers.[45] Therefore, observations of a decrease in the $C_2H_5^\bullet + O_2$ reaction rate with increasing temperature do not imply a corresponding decrease in product yield.

C. Ab Initio Investigations. By 1990 ab initio electronic structure theory had matured to the point where serious theoretical examinations of the ethyl + O_2 reaction were feasible. The first study was that of Skancke and Skancke.[69] Based on Møller−Plesset perturbation theory, their primary results predicted that the barrier for the reverse reaction $C_2H_4 + HO_2^\bullet \rightarrow {}^\bullet CH_2CH_2OOH$ was 11.3 kcal mol^{-1} at the PMP4/6-31G*//UMP2/6-31G* level with zero-point vibrational energy (ZPVE) corrections. However, their $CH_3CH_2OO^\bullet \rightarrow {}^\bullet CH_2CH_2OOH$ barrier was nearly 50 kcal mol^{-1}. That same year, Boyd, Boyd, and Barclay[70] had placed the ethylperoxy radical at about 30 kcal mol^{-1} below $C_2H_5^\bullet + O_2$ with similar levels of theory. Combining these results, it appeared that the overall barrier of M4 was large, about 20 kcal mol^{-1} above reactants.

By 1994 Quelch, Gallo, Schaefer, and co-workers[67,71] (hereafter QGS) had thoroughly investigated the mechanism assumed by Wagner et al.[58] (M4) using configuration interaction and coupled cluster theories. At the CCSD(T)/DZP//CISD/DZP level of theory, QGS[67] found the β-hydrogen transfer barrier to be 9.1 kcal mol^{-1} above reactants with ZPVE corrections. Furthermore, they located the concerted $HO_2^\bullet$ elimination transition state of M5, finding a barrier of only +4.5 kcal mol^{-1}. Yet the

computed barriers in both mechanisms were at odds with the E_a(0 K) value obtained by Wagner et al.[58] of −2.4 kcal mol^{-1}. On the other hand, the consistent application of increasing levels of correlation in their studies [from CISD to CCSD(T)] indicated that both barriers would likely drop with more sophisticated computations (which were impractical at that time). However, the presence of an excited state reaction surface stemming from $C_2H_5^\bullet$ ($\tilde{X}\ ^2A'$) + O_2 ($a\ ^1\Delta_g$) appeared to complicate their results. Among the questionable results was an ethylperoxy β-hydrogen isomerization transition state with an obviously unrealistic imaginary frequency of 4788*i* cm^{-1} at the ROHF-CISD/DZP level.

A few months later, Green[72] reported BLYP/TZVP and BP86/TZVP density functional theory (DFT) predictions. Green found the barrier for the reverse reaction, $C_2H_4 + HO_2^\bullet \rightarrow {}^\bullet CH_2CH_2OOH$, to be 9.6 and 10.8 kcal mol^{-1} with BLYP and BP86, respectively. He also placed this barrier slightly above (about 1.5 kcal mol^{-1}) that for hydroperoxyethyl decomposition into oxirane + $^\bullet$OH. In contrast, Shen, Moise, and Pritchard[73] found the barrier to be slightly below that for decomposition into oxirane + $^\bullet$OH, by 3.3 kcal mol^{-1} at the UMP4//6-31G//UMP2/6-31G level. Shen et al. also placed the α-hydrogen transfer barrier of ethylperoxy at 9.1 kcal mol^{-1} above the β-hydrogen transfer barrier (cf. mechanisms M2, M3, and M4).

In 1997, Ignatyev, Xie, Allen, and Schaefer[74] (hereafter IXAS) studied the three primary mechanisms leading to olefin formation (M1, M4, and M5) with increasing levels of density functional theory, up to UB3LYP/TZ2Pf. They found the overall barrier of M4 to be E_a(0 K) = 8.0 kcal mol^{-1}. Further hindering this mechanism, they also found the corresponding hydroperoxyethyl decomposition barrier to be 1.5 kcal mol^{-1} above reactants. However, IXAS did find the concerted $HO_2^\bullet$ elimination transition state of M5 to lie at −1.9 kcal mol^{-1}, in good agreement with the E_a(0 K) = −2.4 kcal mol^{-1} determined by Wagner et al.[58] The barrier for direct hydrogen abstraction (M1) was E_a(0 K) = +13.5 kcal mol^{-1}.

In summary, by 1997 the theoretical studies of QGS and IXAS seemed to favor concerted elimination of $HO_2^\bullet$ from the ethylperoxy radical, rather than ethylperoxy β-hydrogen transfer, in contrast to the conclusions of most experimental work, though not necessarily at variance with the observations. Furthermore, the work of Pritchard et al.[73] and Green[72] indicated that the barrier for decomposition of $^\bullet CH_2CH_2OOH$ into ethylene is small (around 10 kcal mol^{-1} above products) but competitive with that for decomposition into oxirane, thus leaving the predominance of ethylene formation unexplained if M4 is operative. However, in nearly every theoretical study, questions as to the reliability of the theoretical results may be raised due to either spin contamination in unrestricted wave functions, multireference character in the electronic structure, or intricacies arising from the low-lying excited-state surface.

In this Feature Article we describe high-level coupled cluster ab initio [CCSD and CCSD(T)] theoretical results on every important reactant, intermediate, transition state, and product involved in each of the five mechanisms, M1−M5, with due concern for relevant pitfalls in electronic structure computations. Comparison with experimental evidence is made. Our results provide near-definitive energetics for each mechanism and suggest that the multichanneled oxidation of the ethyl radical is finally, after nearly 100 years, understood.

II. Theoretical Methods

Geometry optimizations were performed using analytic gradient techniques with the coupled cluster method including all single and double excitations [CCSD][75,76] and with CCSD augmented by a perturbative correction for connected triple excitations [CCSD(T)].[77−80] All electrons were correlated, and no virtual orbitals were deleted. A spin-restricted open-shell Hartree−Fock (ROHF) reference was used. Molecular geometries were considered converged when the rms gradient fell below 10^{-6} hartree/bohr. Harmonic vibrational frequencies were computed via finite differences of analytic first derivatives. All computations were performed using the ACES II ab initio program system.[81]

Three basis sets were employed, which are denoted as DZP, TZ2P, and TZ2Pf. The DZP basis set is the standard double-ζ set of Huzinaga and Dunning[82,83] augmented with a set of five d polarization functions on the heavy atoms [α_d(C) = 0.75 and α_d(O) = 0.85] and a set of p functions on the hydrogen atoms [α_p(H) = 0.75]. This basis may be denoted as [C,O (9s5pld/4s2pld) and H (4s1p/2slp)] and results in 85 contracted basis functions for the $C_2H_5^\bullet + O_2$ system.

The TZ2P basis set consisted of the contracted triple-ζ Gaussian functions of Dunning[84] augmented with two sets of five d polarization functions on the heavy atoms [α_d(C) = 1.50 and 0.375, α_d(O) = 1.70 and 0.425] and two sets of p polarization functions on the hydrogen atoms [α_p(H) = 1.5 and 0.375]. This basis set may be denoted as [C,O (10s6p2d/5s3p2d) and H (5s2p/3s2p)] and results in 141 contracted basis functions.

To obtain the TZ2Pf basis set, one set of seven f polarization functions was added to the TZ2P basis for each heavy atom [α_f(C) = 0.80 and α_f(O) = 1.40] and a set of five d polarization functions was appended to each hydrogen atom [α_d(H) = 1.0]. This basis set may be denoted as [C,O (10s6p2d1f/5s3p2d1f) and H (5s2pld/3s2p1d)] and results in 194 contracted basis functions.

To facilitate comparison between the coupled cluster results presented here, the CISD results of QGS[67,71] and the density functional results of IXAS,[74] our DZP basis was chosen to be identical to that of the two earlier studies with the exception that spherical harmonic d functions were used instead of Cartesian d functions. Furthermore, our TZ2Pf basis set is identical to that of IXAS. In a few instances, we report results obtained at the UB3LYP/TZ2Pf level of theory. These results were determined with the Gaussian94 program system[85] in an identical manner to the UB3LYP/TZ2Pf computations of IXAS.

The geometries of all species examined in this study were obtained at both the CCSD/DZP and CCSD(T)/DZP levels. Additional geometries for **TS1**, **TS1′**, and **TS2** were obtained at the CCSD/TZ2P and CCSD(T)/TZ2P levels. The geometries of the reactants (**1**) and products (**5**, **7**, and **8**) were obtained at the aforementioned levels as well as at the CCSD(T)/TZ2Pf level. CCSD/TZ2P and CCSD(T)/TZ2P single-point energies were obtained for all species at the CCSD(T)/DZP geometries. Further, for species optimized at the CCSD(T)/TZ2P level, CCSD(T)/TZ2Pf single-point energies were computed. Harmonic vibrational frequencies were determined at the CCSD/DZP level for all species and at the CCSD(T)/DZP level for **TS1′** and **TS2**.

As alluded to in the Introduction, a few of the species examined here may have appreciable multireference character, which could degrade the quality of the single-reference coupled cluster methods employed in this study. One means of assessing multireference character in coupled cluster methods is through an open-shell T_1 diagnostic. We have implemented the T_1 diagnostic of Jayatilaka and Lee[86] in our PSI 3.0 program package[87] and report T_1 values for several questionable species with the above DZP and/or TZ2P basis sets at the optimized geometries from the ACES II program system.

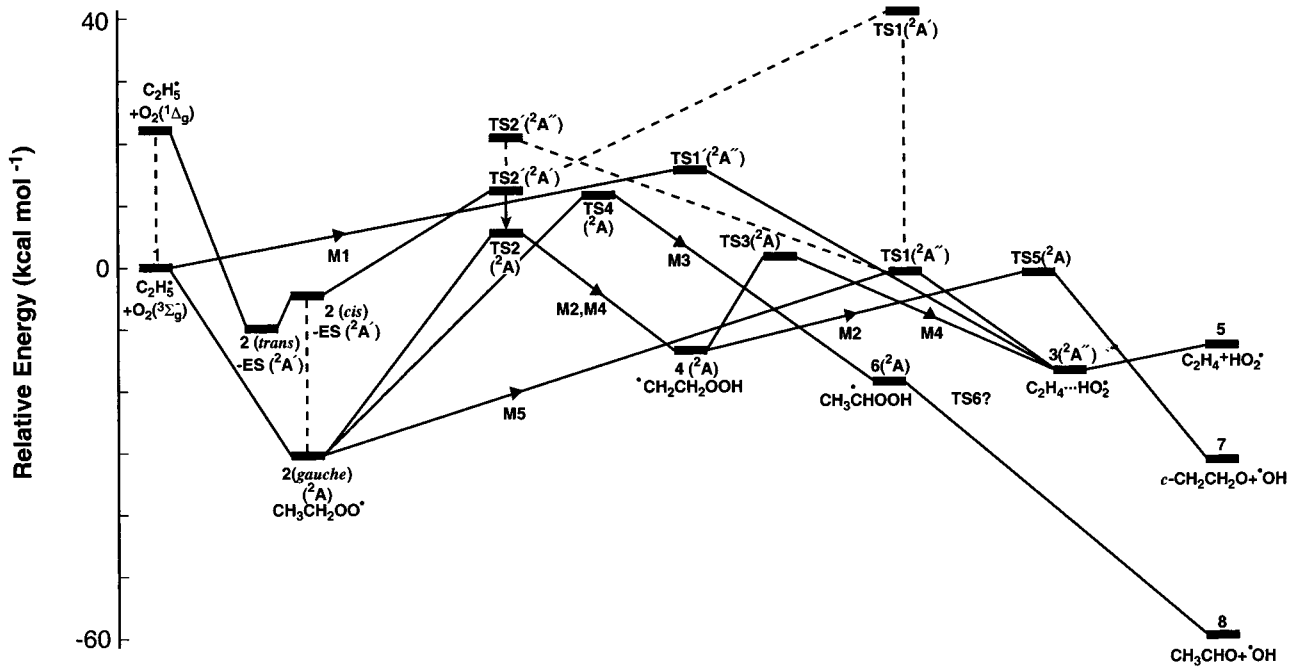

Figure 1. Schematic of the five mechanisms, M1−M5, for the $C_2H_5^{\bullet} + O_2$ reaction. See section III for definitions of each intermediate and transition state. See Figures 2−16 for optimized structures of each species, except **TS6**. All notation is consistent with ref 74.

III. Notation

We have already discussed five mechanisms, M1−M5, for the $C_2H_5^{\bullet} + O_2$ reaction. We rewrite each mechanism here in more detail with notation consistent to that of the earlier work of IXAS.[74]

M1:

$$\underbrace{C_2H_5^{\bullet} + O_2}_{1} \rightarrow TS1' \rightarrow \underbrace{C_2H_4\cdots HO_2^{\bullet}}_{3} \rightarrow \underbrace{C_2H_4 + HO_2^{\bullet}}_{5}$$

M2:

$$1 \rightarrow \underbrace{CH_3CH_2OO^{\bullet}}_{2} \rightarrow TS2 \rightarrow \underbrace{{}^{\bullet}CH_2CH_2OOH}_{4} \rightarrow TS5 \rightarrow \underbrace{c\text{-}CH_2CH_2O + {}^{\bullet}OH}_{7}$$

M3:

$$1 \rightarrow \underbrace{CH_3CH_2OO^{\bullet}}_{2} \rightarrow TS4 \rightarrow \underbrace{CH_3\dot{C}HOOH}_{6} \rightarrow TS6 \rightarrow \underbrace{CH_3CHO + {}^{\bullet}OH}_{8}$$

M4:

$$1 \rightarrow \underbrace{CH_3CH_2OO^{\bullet}}_{2} \rightarrow TS2 \rightarrow \underbrace{{}^{\bullet}CH_2CH_2OOH}_{4} \rightarrow TS3 \rightarrow \underbrace{C_2H_4\cdots HO_2^{\bullet}}_{3} \rightarrow \underbrace{C_2H_4 + HO_2^{\bullet}}_{5}$$

M5:

$$1 \rightarrow \underbrace{CH_3CH_2OO^{\bullet}}_{2} \rightarrow TS1 \rightarrow \underbrace{C_2H_4\cdots HO_2^{\bullet}}_{3} \rightarrow \underbrace{C_2H_4 + HO_2^{\bullet}}_{5}$$

In Figure 1 and the cover illustration, the energetics of each species **1**−**8** and all transition states (**TS1**−**TS6**) for Ml−M5 are pictured relative to the ground state reactants, **1**. Actual energetic values at all levels of theory are listed in Table 5. All species are pictured individually in Figures 2−16 with optimized geometries at various levels of theory.

IV. Quality of Coupled Cluster Results

A. Geometric Structures. Experimentally determined geometries are available for each reactant and product except the ethyl radical. With all geometric parameters, independent of whether experimentally derived values are r_e, r_0, or r_m parameters, agreement between the CCSD(T)/TZ2Pf optimized geometries (see Figures 2, 7, and 13) and experimental values are within 0.01 Å for bond lengths and 1.0° for bond angles. The only exception is the HCH angle in acetaldehyde, which theory underestimates by 1.9°. Agreement is nearly as good at the CCSD(T)/TZ2P level, and only slightly worse at the CCSD(T)/DZP level. Furthermore, our best geometry of ethylene (Figure 7) agrees within 0.002 Å and 0.12° of values obtained by Martin

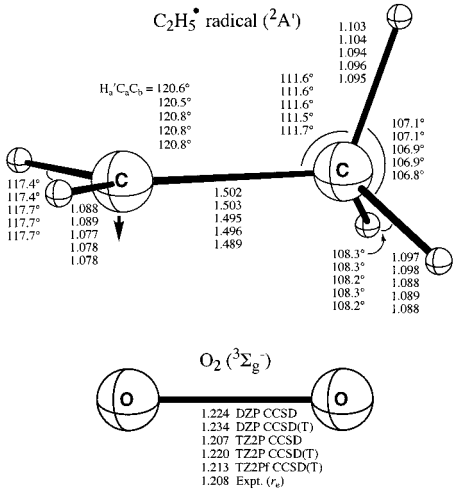

1
Reactants

Figure 2. Optimized geometries at various levels of theory, listed in order, of the reactants (**1**), ethyl radical and oxygen. In all structures in this paper, distances are given in Å and bond angles in degrees. The experimental r_e value for oxygen is from ref 92. An experimentally vibrationally averaged C−C bond distance of 1.492 ± 0.002 Å has been reported for the ethyl radical in ref 90. The notation in this and all subsequent figures is identical to that of ref 74 and assumes a connectivity in which (C_a, C_b) are the (methylene, methyl) carbons in the $C_2H_5^{\bullet}$ group, (O_a, O_b) are (linking, terminal) oxygens in the O_2 moiety, (H_b, H_b', H_b'') are the (in, above, below)-the-plane methyl hydrogens, and (H_a', H_a'') are the (above, below)-the-plane methylene hydrogens. The reaction proceeds as O_a bonds to C_a, O_b abstracts H_b, and then $H_bO_b-O_a$ separates from $(H_a')(H_a'')C_a{=}C_b(H_b'')(H_b')$. In certain cases, the direction of pyramidalization about an apex carbon is indicated by a heavy arrow to avert structural ambiguity.

and Taylor:[88] r_e(CC) = 1.3307(3) Å, r_e(CH) = 1.0809(3) Å, and θ_e(HCH) = 117.12(3), which approximate the complete-basis, all-electron CCSD(T) limit. Additionally, earlier work[89] has shown that the $C_2H_5^\bullet$ geometry pictured in Figure 2 is the lowest-energy minimum structure of the ethyl radical, and recent experimental laser spectroscopy results[90] suggest a vibrationally averaged C−C bond distance of 1.49 Å, in excellent agreement with our CCSD(T)/TZ2Pf distance of 1.489 Å.

Although experimental geometries are not known for any of the intermediates of Ml−M5, the CCSD(T)/DZP geometries of each intermediate are in qualitative agreement with previous UB3LYP/TZ2Pf and CISD/DZP geometries[67,71,74] (most bond distances and angles agree to within 0.03 Å and 1.5°). For crucial transition states, we have optimized the geometries at the CCSD/TZ2P and CCSD(T)/TZ2P levels. We do not generally discuss geometries of the intermediates or transition states here, but as each mechanism is presented, we do highlight the most salient structural features and note where significant deviations from previous theoretical results arise.

B. Vibrational Frequencies. Determination of coupled cluster harmonic vibrational frequencies is possible only via finite differences of analytical first derivatives in the version of the ACES II program suite available to us at the time of this study. Many of the intermediates in this study are structurally asymmetric (i.e., belong to the C_1 point group) and require as many as 42 displacements for a frequency determination. Such a computation requires a large amount of CPU time (on the order of one month), even at the CCSD/DZP level. Thus, obtaining frequencies at a higher level of theory is impractical at this time. Nonetheless, it is prudent to assess the quality of our CCSD/DZP frequencies. (Computed harmonic frequencies are available in Supporting Information.)

Experimental harmonic frequency values are available only for ethylene,[91] O_2,[92] and $^\bullet$OH.[92] Comparing our CCSD/DZP harmonic frequencies to these values, we find excellent agreement, with an average absolute percent error from experiment of only 1.7% and a maximum error of 3.8%, excluding the trans b_{2g} CH_2 wag mode (ω_8) of ethylene. Previous work[88,93−95] has shown that ω_8 is sensitive to diradical character in the wave function as well as polarization functions, and improving either basis set or method, e.g., to the CCSD(T)/TZ2Pf level, should improve the quality of the computational results for ω_8.

Experimental fundamental frequencies are available for oxirane,[96] acetaldehyde,[96] ethyl radical,[97−99] hydroperoxy radical,[100] and the ethylperoxy radical.[98] Together, this set constitutes 43 frequencies. Comparing our CCSD/DZP harmonic vibrational frequencies[101] to 41 of these anharmonic frequencies gives an average absolute percent error from experiment of 4.5% with a maximum percent error of 8.5%. The excluded frequencies are the asymmetric CH_3 rocking mode of acetaldehyde (ν_{13}) and the CH_2 pyramidal bending mode of the ethyl radical (ν_9). Our computed harmonic frequency for the former mode is 1151 cm^{-1} while the experimental fundamental value is only 867 cm^{-1}. To further test our computed value, we also determined frequencies for acetaldehyde at the UB3LYP/TZ2Pf level, which gives a value of 1137 cm^{-1}. Thus, it appears that the experimental value in this case may be in error. The ν_9 mode of $C_2H_5^\bullet$, which is 540 cm^{-1} from experiment,[97−99] is consistently underestimated by theory: 458 cm^{-1} with UMP2/6-311G**,[99] 494 cm^{-1} with UB3LYP/TZ2Pf,[74] and 464 cm^{-1} in this work (CCSD/DZP). Additionally, we investigated the effects of a scaling factor on our CCSD/DZP harmonic frequencies. A scale factor of 0.95 substantially improves agreement with experimental fundamentals with an average absolute percent error of only 2.5%. However, zero-point vibrational energy (ZPVE) corrections computed with accurate theoretical harmonic frequencies are in principle more representative of the true molecular ZPVE if scaling to experimental fundamentals is not employed.[102] Thus we have not scaled our ω_i values in arriving at ZPVE corrections.

TABLE 1: Experimentally Derived Heats of Formation at 0 K ($\Delta_f H_0$, kcal mol^{-1}) for Various Species in the $C_2H_5^\bullet + O_2$ Reaction System

species	$\Delta_f H_0$	ref
$C_2H_5^\bullet$	31.5 ± 0.5	129[a]
C_2H_4	14.58 ± 0.07	130
$HO_2^\bullet$	4.2 ± 0.5[b]	112, 115
$^\bullet$OH	9.18 ± 0.29	130
c-CH_2CH_2O	−9.59 ± 0.15	130
CH_3CHO	−37.5 ± 0.1[c]	131

[a] High-level ab initio results give 31.4 ± 0.5 kcal mol^{-1} (ref 132). These results include CH_2 internal rotation effects (refs 133−135). [b] Estimated by using the recommended $\Delta_f H_{298}$ value of 3.5 ± 0.5 kcal mol^{-1} and applying a −0.7 kcal mol^{-1} harmonic adjustment for [$\Delta_f H_{298} - \Delta_f H_0$]. The adjustment was determined using CCSD/DZP harmonic frequencies and includes translational, rotational, and vibrational corrections. Electronic contributions are negligible. [c] Estimated by using the recommended $\Delta_f H_{298}$ value of −39.7 ± 0.1 kcal mol^{-1} and applying a −2.6 kcal mol^{-1} harmonic adjustment for [$\Delta_f H_{298} - \Delta_f H_0$] (determined as in $HO_2^\bullet$) and a +0.4 kcal mol^{-1} hindered rotor correction (refs 136, 137) based on the experimentally known barrier to rotation (refs 138, 139) of 408 cm^{-1} and our CCSD(T)/TZ2Pf geometry.

C. Thermodynamic Considerations. Although the CCSD(T)/TZ2Pf-optimized geometries of reactants and products were the most accurate, optimizations of all intermediates and transition states at this level of theory are prohibitive due to the size of the CCSD(T) computations and the number of species involved in the five mechanisms. Fortunately, full CCSD(T)/TZ2Pf optimizations prove to be unnecessary. In Table 1 we report $\Delta_f H_0$ literature values for each reactant and product. It has only been within the past few years that accurate experimentally based determinations of these $\Delta_f H_0$ values for all species have become known. We consider only reactants and products here, as heats of formation (even at 298 K) for the intermediates involved in the five mechanisms are less well-known, if at all. In Table 2, we compare the heats of reaction at 0 K ($\Delta_r H_0$) to those obtained at three levels of theory. At the CCSD(T)/TZ2Pf and CCSD(T)/TZ2Pf//CCSD(T)/TZ2P levels, computed values for each $\Delta_r H_0$ are within 0.5 kcal mol^{-1} of the literature values and certainly within expected experimental error limits. Indeed, the same is true at the CCSD(T)/TZ2P//CCSD(T)/DZP level, excepting $\Delta_r H_0$ for production of oxirane + $^\bullet$OH.

The previous ab initio computations of QGS[67] and IXAS[74] place the $C_2H_5^\bullet + O_2 \rightarrow C_2H_4 + HO_2^\bullet$ reaction enthalpy at −8.5 and −11.2 kcal mol^{-1} with the CCSD(T)/DZP//CISD/DZP and UB3LYP/TZ2Pf methods, respectively. Clearly, our present energetics in Table 2 are a significant improvement over previous studies. It should also be noted that Wagner et al.[58] obtained an experimentally derived value of −13.0 kcal mol^{-1} for this same reaction, in good agreement with our results and those derived from experimental $\Delta_f H_0$ values.

Because the CCSD and CCSD(T) methods are size-extensive, it can be expected that the accuracy seen in the reactants and products will be similar for the intermediate species within each mechanism. Transition states, however, may be somewhat less accurate. Nonetheless, we expect from the results in Table 2 that at the CCSD(T)/TZ2P//CCSD/DZP level energetics of the ethyl + O_2 reaction are probably accurate to within ±3.0 kcal mol^{-1} and those at the CCSD(T)/TZ2Pf//CCSD(T)/TZ2P level

TABLE 2: Heats of Reaction at 0 K ($\Delta_r H_0$, kcal mol^{-1}) for the $C_2H_5^\bullet + O_2$ System

products	CCSD(T)/TZ2P// CCSD(T)/DZP[a]	CCSD(T)/TZ2Pf// CCSD(T)/TZ2P[a]	CCSD(T)/ TZ2Pf[a]	expt[b]
$C_2H_4 + HO_2^\bullet$	−13.0	−12.8	−12.8	−12.7
c-$CH_2CH_2O + {}^\bullet OH$	−29.9	−31.4	−31.5	−31.9
$CH_3CHO + {}^\bullet OH$	−60.1	−59.6	−60.1	−59.8

[a] Theoretical values include CCSD/DZP ZPVE corrections. [b] Computed from values in Table 1.

are accurate to within ±1.5 kcal mol^{-1}. A possible caveat to this surmisal would be unreliable coupled cluster wave functions resulting from the multireference nature of a particular species. We find only one significant instance of this, which we discuss next. In the remainder of our discussion we report only the CCSD(T)/TZ2P//CCSD(T)/DZP (ZPVE-corrected) values, unless otherwise noted, and for comparison, quote only ZPVE-corrected values from previous studies, when possible.

D. Electronic Considerations. Unrestricted electronic structure wave functions are not eigenfunctions of the S^2 operator and hence may give $\langle S^2\rangle$ values in error from the true $\langle S^2\rangle = 0.75$ for doublet species. In the work of Skancke and Skancke,[69] they report an $\langle S^2\rangle$ value of 1.02 for **TS3** at the UHF/6-31G* level. Likewise, with UMP2/TZ2P theory, Green[72] reports an $\langle S^2\rangle$ value of 1.04 for **TS3**, an even higher value of 1.31 for **TS5**, and value of 0.80 for **TS2**. In an effort to avoid such large contamination from higher spin states, other theoretical studies[67,71,73] have used an ROHF formalism or unrestricted density functional methods, which usually suffer less from spin contamination than conventional ab initio methods. In the work of IXAS, **TS3** has the largest $\langle S^2\rangle$ value (0.78) of all species using unrestricted DFT.[74]

In addition to spin contamination concerns, in the studies of QGS[67,71] the importance of an excited-state surface originating from the $C_2H_5^\bullet$ ($\tilde{X}\ ^2A'$) + O_2 (a $^1\Delta_g$) reaction was recognized. Alongside concerns stemming from this energetically low-lying surface, QGS suspected that some of the species involved in ethyl oxidation may not be well treated with a single-reference based wave function. To test this suspicion, QGS reported T_1 diagnostic values obtained at the CCSD/DZP//CISD/DZP level. The T_1 diagnostic gives a qualitative assessment of the significance of nondynamical (or static) correlation: the larger the T_1 value, the less reliable the results of the single-reference coupled cluster wave function. However, the T_1 analysis of QGS was based on the closed-shell formalism of Lee and coworkers,[103,104] which cannot be directly applied to open-shell coupled cluster wave functions.

We report T_1 diagnostic values using the open-shell T_1 formalism of Jayatilaka and Lee[86] in Table 3. This open-shell diagnostic is consistent with that for closed-shell systems and is size-extensive. However, few results employing this diagnostic have been reported in the literature, and thus it is unclear what exactly constitutes a "large" T_1 value for open-shell systems. Jayatilaka and Lee suggest that open-shell T_1 values may be larger than those of closed-shell systems, where T_1 values greater than 0.02 are typically suspect.[104]

Our T_1 value for $HO_2^\bullet$ ($^2A''$) is 0.034 at both the CCSD/DZP and CCSD(T)/TZ2P levels. Previous theoretical work indicates that coupled cluster theory can very reliably treat the HO_2 radical.[105,106] Additionally, we have already discussed that the geometry and energetics of the HO_2 radical are in good agreement with experimental values (see above sections). Hence we have every reason to trust our CCSD and CCSD(T) results for $HO_2^\bullet$. In addition, we also computed T_1 values for the cyano radical (CN) at the CCSD/DZP and CCSD(T)/TZ2P levels. The cyano radical is notorious for having large spin contamination with unrestricted methods (UHF, UMP2).[107] Studies using coupled cluster methods have shown that CCSD and CCSD(T) overcome problems associated with spin contamination and reliably reproduce experimental properties of CN.[108−110] Our T_1 values for CN are 0.045 and 0.044 with CCSD/DZP and CCSD(T)/TZ2P, respectively. We will use these values as a "benchmark" for species in this study—those with T_1 values above 0.044 will be considered somewhat less reliable.

TABLE 3: Open-Shell T_1 Diagnostic Values for Various Species in the $C_2H_5^\bullet + O_2$ System Compared to the Cyano Radical

species	CCSD/DZP[a]	CCSD(T)/TZ2P[a]
$HO_2^\bullet$	0.034	0.034
TS1	0.033	0.032
TS1′	0.058	0.047
TS2	0.028	0.025
TS2′	0.018	
TS3	0.043	0.033[b]
TS4	0.016	
TS5	0.042	0.040[b]
CN	0.045	0.044

[a] T_1 value computed at this optimized geometry. [b] T_1 value computed with the TZ2P basis at the CCSD(T)/DZP geometry.

Examining Table 3, we see that all species have T_1 values below the 0.034 value of $HO_2^\bullet$ except **TS1′**, **TS3,** and **TS5**. However, the T_1 values of the latter two species are still below those of our CN benchmark. Although the T_1 value of **TS1′** drops from 0.058 at CCSD/DZP to 0.047 at CCSD(T)/TZ2P, it remains above the T_1 values of CN. Thus, our computed results for **TS1′** may not be entirely reliable, though surely not unreasonable. Fortunately, the energetics of **TS1′** are of lesser importance to this study. Of more concern are the energetics of **TS3** and **TS5**. We find T_1 values of 0.043 and 0.042 at CCSD/DZP for **TS3** and **TS5**, respectively. Although we did not optimize either **TS3** or **TS5** at the CCSD(T)/TZ2P level, single-point CCSD/TZ2P wave functions give T_1 values of 0.040 (**TS5**) and only 0.033 (**TS3**), both below the benchmark value of 0.044, indicating that coupled cluster theory should overcome multireference concerns for **TS3** and **TS5**. It is clear then that for all species except **TS1′** our CCSD and CCSD(T) results should be quite reliable and can be expected to yield energetics of similar quality to those discussed for the reactant and product species in the preceding section. We also note in this regard that the largest absolute t_2 amplitude occurs in **TS1′** with a magnitude of 0.17. For all other species in this study the t_2 amplitudes are less (and in most instances significantly less) than the largest t_2 amplitude in ethylene, 0.11.

V. Discussion and Analysis of the $C_2H_5\bullet + O_2$ Reaction

A. Ethylperoxy Radical. The initial step in each of M2−M5 involves formation of the ethylperoxy radical, **2** (cf. eq 5). Previous work of QGS[71] and IXAS[74] investigated rotamers of **2** about the C−O bond. We likewise have examined these rotamers and present a summary of our results and previous work in Table 4. We label the four rotamers of the ethylperoxy radical as **2**(*gauche*), **2** (*gauche*-**TS**), **2**(*trans*), and **2**(*cis*-**TS**)

TABLE 4: Vibrationless Relative Energies (in kcal mol^{-1}) of Four Ground-State (^{2}A″ or ^{2}A) and Excited-State (^{2}A′) Ethylperoxy Radical Rotamers As Depicted in Figures 3, 4, and 8

rotamer	CISD+Q/DZP[a]	B3LYP/TZ2Pf[b]	CCSD(T)/DZP	CCSD(T)/TZ2P[c]	Hessian index[d]
^{2}A gauche	0.0	0.0	0.0	0.0	0
^{2}A gauche-**TS**	1.0	0.7	1.2	1.2	1
^{2}A″ trans	0.1	0.01	0.3	0.2	0
^{2}A″ cis-**TS**	2.6	2.1	2.4	2.5	1
^{2}A′ trans	17.4	21.8	20.6	20.6	0
^{2}A′ cis[e]	23.0	27.4	26.0	26.4	0

[a] Reference 71. [b] Reference 74. [c] Evaluated at the CCSD(T)/DZP geometry. [d] The number of imaginary vibrational frequencies. [e] This species is a transition state at the CISD and B3LYP levels.

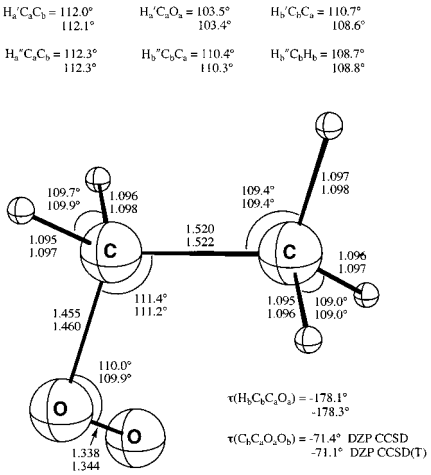

2 (*gauche*)
^{2}A (C$_1$)

Figure 3. Optimized geometries of the ethylperoxy radical (**2**) in the gauche conformation. See caption of Figure 2 for an explanation of the assumed notation. See also ref 111.

based on the orientation of the O−O and C−C bonds, each being illustrated in Figures 3 and 4.[111] The structural parameters of each of these rotamers are in close agreement with the corresponding B3LYP/TZ2P geometries of IXAS.[74] All four species are within 2.5 kcal mol^{-1} of one another, revealing that rotation about the C−O bond is easily achieved and facilitates rearrangements of the ethylperoxy radical. Because the **2**(*gauche*) conformation of the ethylperoxy radical is the lowest-energy rotamer, we refer to it simply as **2**.

The enthalpy of reaction for eq 5, which is equivalent to the negative of the R−$O_2^•$ bond energy, has long been of interest as a reference point for understanding larger peroxy radicals.[112] The first experimental estimate of $\Delta_rH°_{298}$ was given by Slagle, Ratajczak, and Gutman[46] in 1986, with a value of -35.2 ± 1.5 kcal mol^{-1}. In 1998, Knyazev and Slagle[113] reanalyzed the 1986 data and obtained $\Delta_rH°_{298} = -35.5 \pm 2.0$ kcal mo1^{-1}. The value in both studies is derived from six K_p data points for temperatures between 609 and 654 K. A $\Delta_rH°_{298}$ is then extracted by applying appropriate thermodynamic corrections. In the 1998 work, these corrections were derived from experimental data combined with ab initio results from the studies of QGS.[71] The 1990 study of Wagner et al.[58] corrected the 1986 value, $\Delta_rH°_{298} = -35.2 \pm 1.5$ kcal mol^{-1}, to 0 K: $\Delta_rH_{298} - \Delta_rH_0 = -1.2$ kcal mo1^{-1}. This Δ_rH_0 was then adjusted within the experimental error of ±1.5 kcal mol^{-1} in their RRKM model to obtain a final $\Delta_rH_0 = -32.9 \pm 0.5$ kcal mol^{-1}.

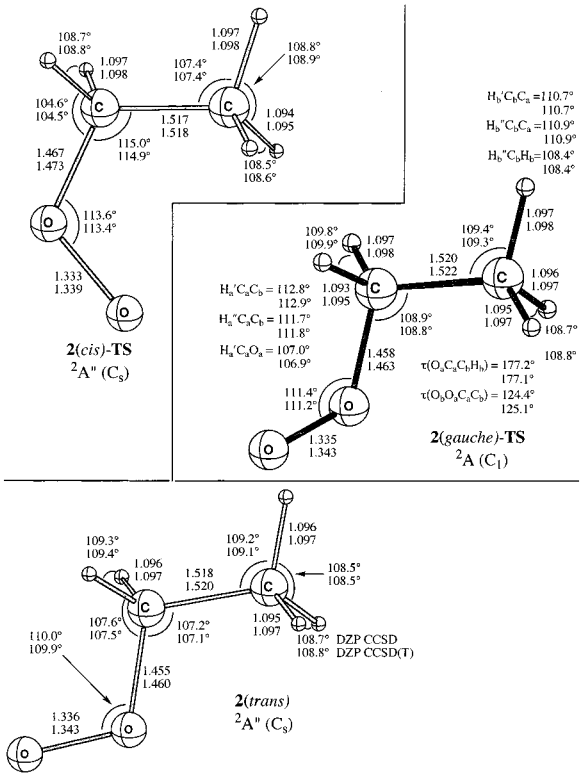

Figure 4. Optimized geometries of the ethylperoxy radical in the cis, gauche, and trans conformations. Note that **2**(*gauche*-**TS**) interconverts **2**(*gauche*) (Figure 3) with **2**(*trans*) and that **2**(*cis*-**TS**) interconverts **2**(*gauche*) with its mirror image. See caption of Figure 2 for an explanation of the assumed notation. See also ref 111.

On the other hand, all theoretical values[67,70,74] for Δ_rH_0, including our best CCSD(T)/TZ2P//CCSD(T)/DZP value of −30.3, are greater than −31.0 kcal mol^{-1} and thus greater than the $\Delta_rH_0 = -32.9$ derived by Wagner et al.[58] However, if we assume Wagner et al.'s $\Delta_rH_{298} - \Delta_rH_0$ enthalpy correction of −1.2 kcal mol^{-1} and use our $\Delta_rH_0 = -30.3$, we obtain $\Delta_rH°_{298} = -31.5$ kcal mol^{-1}. This is in reasonable agreement with the recently computed B3LYP/6-311+G(2df,2p) $\Delta_rH°_{298} = -30.1$ kcal mol^{-1} obtained by Brinck, Lee, and Jonsson[114] and nearly matches the best value obtained from the group additivity method of -31.3 ± 1.1 kcal mol^{-1}.[112,115]

Including previous work of QGS,[67,71] we have a sequence of theoretical Δ_rH_0 values (in kcal mol^{-1}, see Table 6) which seems to have converged: −27.0 [CISD/DZP], −28.0 [CISD+Q/DZP], −29.9 [CCSD/DZP], −30.5 [CCSD(T)/DZP], −30.3 [CCSD(T)/TZ2P//CCSD(T)/DZP]. It appears that the true Δ_rH_T values at $T = 0$ K and $T = 298$ K may be greater than −31.0 and −33.0 kcal mol^{-1}, respectively, i.e., current empirical values for the $CH_3CH_2-O_2$ binding energy are too large. Certainly, errors of a few kcal mol^{-1} can be accounted for in the experimental data due to the limited number of data points and the thermodynamic corrections employed, which account for only one conformer of the ethylperoxy radical and which use some scaled ROHF/DZP frequencies. More ab initio data is also warranted, because it is well-known that definitive bond- energies cannot generally be obtained without including multiple, higher-order polarization manifolds in the basis set.

B. Energetics of Each Mechanism. *1. Direct Hydrogen Abstraction from the Ethyl Radical by O_2 (M1).* Although the simplest mechanism, direct bimolecular hydrogen abstraction was only first studied by ab initio methods in the previous work of IXAS.[74] In their work a C_s, ^{2}A″ transition state, **TS1′**, was

TABLE 5: Relative Energies (in kcal mol^{-1}) of the Intermediates, Transition States, and Products Involved in the $C_2H_5^\bullet + O_2$ Reaction (Species Common to One or More Mechanisms Are Listed Only Once)

species[a]	CCSD/ DZP	CCSD(T)/ DZP	CCSD/TZ2P single point[c]	CCSD(T)/TZ2P single point[c]	CCSD/ TZ2P	CCSD(T)/ TZ2P	CCSD(T)/TZ2Pf single point[d]	ΔZPVE[b]
reactants								
$C_2H_5^\bullet + O_2$ (**1**)	0.0	0.0	0.0	0.0	0.0	0.0	0.0	0.0
mechanism M1								
TS1′	28.7	18.3	26.6	16.8	28.8	16.9	16.4	−1.3[e]
3	−13.8	−14.7	−17.9	−19.0				2.1
$C_2H_4 + HO_2^\bullet$ (**5**)	−9.4	−9.8	−13.3	−13.8	−13.1	−13.8	−13.6[f]	0.8
mechanism M2								
2	−35.5	−36.1	−35.3	−35.9				5.6
TS2	9.8	7.0	9.0	5.5	9.7	5.7	3.7	1.6
4	−14.3	−14.6	−16.6	−17.1				3.4
TS5	6.4	2.3	3.0	−2.0				2.2
c-$CH_2CH_2O + {}^\bullet OH$ (**7**)	−30.2	−29.1	−33.1	−31.6	−32.6	−31.5	−33.1[f]	1.7
mechanism M3								
TS4	14.9	11.3	14.9	10.3				1.2
6	−19.3	−20.1	−21.2	−22.3				3.9
$CH_3CHO + {}^\bullet OH$ (**8**)	−58.6	−57.6	−62.1	−60.7	−61.9	−60.7	−60.2[f]	0.6
mechanism M4								
TS3	7.0	3.8	2.7	−1.1				2.5
mechanism M5								
TS1	7.3	1.9	5.1	−1.2	5.5	−1.2	−2.3	1.4
other species								
2(*trans*)	−35.3	−35.8	−35.2	−35.7				5.5
2(*cis*-**TS**)	−32.9	−33.7	−32.7	−33.4				5.4
2(*gauche*-**TS**)	−34.2	−34.9	−34.1	−34.7				5.4
2(*cis*-ES)	−9.8	−10.1	−9.6	−9.5				5.2
2(*trans*-ES)	−15.4	−15.5	−15.5	−15.3				5.2
TS2′	15.1	12.2	14.7	11.3				0.9[e]
4′	−13.9	−14.3	−16.1	−16.7				3.6
TS3′	8.0	4.5	4.2	−0.2				2.5

[a] See Figures 2−16 for structural depictions. [b] ZPVE corrections are computed at the CCSD/DZP level (imaginary frequencies of transition states are ignored). [c] Evaluated at the CCSD(T)/DZP geometry. [d] Evaluated at the CCSD(T)/TZ2P geometry. [e] Two imaginary frequencies ignored. See text. [f] CCSD(T)/TZ2Pf full optimizations of reactants, **1**, and products, **5**, **7**, and **8**, place the products 13.6, 33.2, and 60.7 kcal mol^{-1} below **1**, respectively.

TABLE 6: A Comparison of Relative Energies (in kcal mol^{-1}, with ZPVE) Obtained by Different Levels of Theory for Species in Three Pathways, Ml, M4, and M5, of the $C_2H_5^\bullet + O_2$ Reaction Leading to $C_2H_4 + HO_2^\bullet$ Formation

species	CISD+Q/DZP[a]	CCSD(T)/DZP// CISD/DZP[a]	B3LYP/ TZ2Pf[b]	CCSD(T)/ DZP[c]	CCSD(T)/TZ2P// CCSD(T)/DZP[c]	CCSD(T)/TZ2Pf// CCSD(T)/TZ2P
$C_2H_5^\bullet + O_2$ (**1**)	0.0	0.0	0.0	0.0	0.0	0.0
2	−28.0	−30.5	−29.0	−30.5	−30.3	
3	−8.7	−12.2	−14.0	−12.6	−16.9	
4	−10.6	−10.3	−9.9	−11.2	−13.7	
TS1	13.3	4.5	−1.9	3.3	0.2	−0.9
TS1′			10.2[d]	17.0	15.5	15.1
TS2	14.8	9.1	8.0	8.6	7.1	5.3
TS3			1.5	6.3	1.4	
$C_2H_4 + HO_2^\bullet$ (**5**)	−5.5	−8.5	−11.2	−9.0	−13.0	−12.8

[a] ZPVE corrections are at the ROHF level and are scaled by 0.91. All values from ref 67. [b] ZPVE corrections are at the B3LYP/DZP level. All values from ref 74. [c] ZPVE corrections are at the CCSD/DZP level. [d] Not adjusted for zero-point vibrational energy.

located which connected the ground-state reactants with a loosely bound $C_2H_4 \cdots HO_2^\bullet$ complex, **3**. This transition state is shown in Figure 5. Our geometry for **TS1′**, optimized at the CCSD(T)/TZ2P level, is consistent with the B3LYP/DZP and B3LYP/TZ2Pf geometries of IXAS, though the $C_b-H_b-O_b$ transition angle is about 12° smaller. Likewise, our geometry for the loose complex **3** (see Figure 6) is consistent with the B3LYP/TZ2Pf geometry of IXAS,[74] and even the long C···H distances are within 0.03 Å of the DFT values. We find that **3** is 3.9 kcal mol^{-1} below the $C_2H_4 + HO_2^\bullet$ products, which is somewhat more bound than the 2.0 kcal mol^{-1} predicted by IXAS.

At the B3LYP/DZP level, IXAS found C_s **TS1′** to be a second-order stationary point with a 32*i* cm^{-1} a″ mode leading to a C_1 transition state. However, using B3LYP/TZ2Pf they found the C_s structure to be a true transition state, albeit with an a″ mode of only 11 cm^{-1}. Like B3LYP/DZP, our methods show the C_s structure to be a saddle point with an a″ imaginary frequency of 32*i* cm^{-1} with CCSD/DZP and 36*i* cm^{-1} with CCSD(T)/DZP. The a′ imaginary frequency is quite large in magnitude, being 3567*i* and 2528*i* cm^{-1} at these levels, respectively, indicating both a thin barrier and a small reduced mass for hydrogen abstraction. The difference of more than 1000 cm^{-1} correlates with a decrease in barrier height of more than 10 kcal mol^{-1} between the CCSD and CCSD(T) methods (see Table 5 and cf. discussion of **TS2** in the next section). Although the CCSD(T)/DZP value of 2528*i* cm^{-1} is reasonable, it is still large compared to the B3LYP/TZ2Pf value of 1681*i* cm^{-1} and may indicate that our computed barrier is somewhat high. As frequency determination with a TZ2P basis set is fairly demanding, we have not investigated frequencies for **TS1′** at higher levels of theory. Nonetheless, the results of IXAS indicate

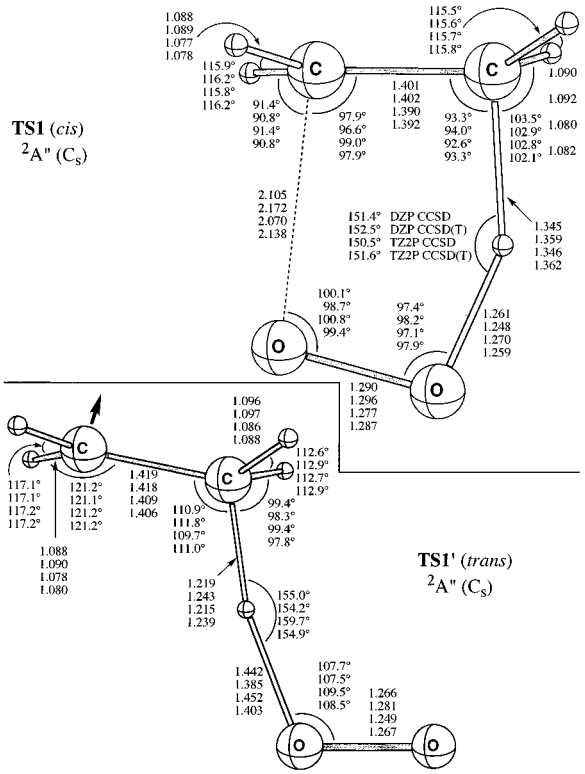

Figure 5. Optimized geometries of the transition state (**TS1**) for concerted elimination of $HO_2^\bullet$ from the ethylperoxy radical (**2**) and of the transition state for direct hydrogen abstraction (**TS1′**). See caption of Figure 2 for an explanation of the assumed notation.

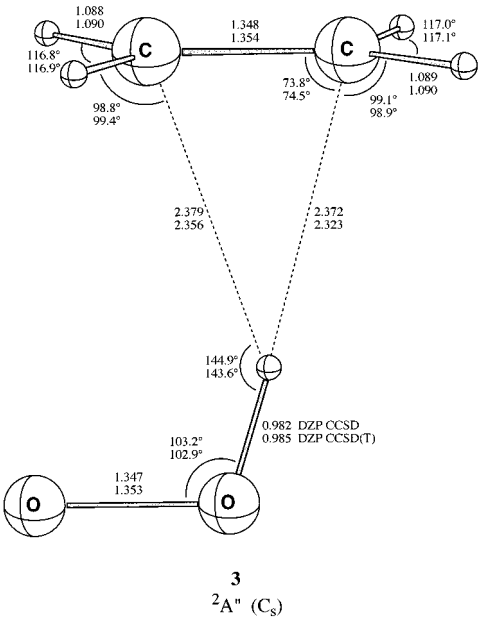

Figure 6. Optimized geometries of the loosely bound $C_2H_4\cdots HO_2^\bullet$ complex (**3**).

that the C_s structure may be a true transition state. Furthermore, at the B3LYP/DZP level, the C_1 transition state located by IXAS is only slightly nonplanar and just 0.008 kcal mol^{-1} below the C_s structure, suggesting that even if the symmetry of **TS1′** is not C_s, the true asymmetric structure would be nearly structurally and energetically equivalent to that pictured in Figure 5. Additionally, our computed structures for **TS1′** are vibrationless structures and not the zero-point averaged structures, which may indeed be effectively of C_s symmetry.

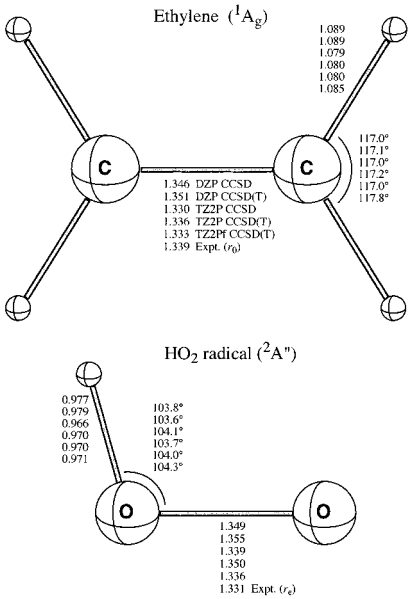

Figure 7. Optimized geometries of the products (**5**), ethylene and the hydroperoxy radical. Experimental r_0 values for ethylene are from ref 125. Theoretical r_e values which approximate the complete-basis, all-electron CCSD(T) limit are r_e(CC) = 1.331 Å, r_e(CH) = 1.081 Å, and θ_e(HCH) = 117.1° (see refs 88 and 95). Experimental r_e values for the hydroxyl radical are from refs 100 and 126.

As already noted in section IV, part D a problem with our coupled cluster computations of **TS1′** is the sizable multireference character of the wave function, which perhaps diminishes the reliability of the computed energetics (and vibrational frequencies) for this transition state. Notwithstanding the difficulties of determining the symmetry or asymmetry and obtaining a reliable reference for **TS1′**, we have obtained energetics for this transition state at the CCSD(T)/TZ2Pf//CCSD(T)/TZ2P level. We predict the transition state to be 15.1 kcal mol^{-1} above the ground-state reactants. This result shows that the barrier for the direct hydrogen abstraction mechanism is larger than most early estimates of this barrier of 3−10 kcal mol^{-1}.[34−41,44,116] At the B3LYP/TZ2Pf level, IXAS[74] find **TS1′** to be 10.2 kcal mol^{-1} above reactants without zero-point correction—considerably lower than our vibrationless value of 16.4 kcal mol^{-1}. We note here that this is the only instance in which the B3LYP/TZ2Pf results of IXAS[74] are significantly (>4 kcal mol^{-1}) lower (or even different) than our best coupled cluster results. Taking the uncertainty in our CCSD(T) results for **TS1′** into account, we feel the actual barrier is likely in the 13 ± 3 kcal mol^{-1} range.

In their assessment of the $C_2H_5^\bullet + O_2$ reaction, Wagner et al.[58] argue that experimental evidence suggests an M1 barrier significantly above the ≈5 kcal mol^{-1} barrier observed for many hydrogen abstraction mechanisms.[117] Wagner et al. note that in the $C_2H_5^\bullet + O_2$ abstraction mechanism not only must the bonds about the migrating hydrogen be broken and formed, but the π bond in O_2 must also be broken, which raises the activation energy above that for most simple abstraction reactions. In summary, we conclude with confidence that the barrier for M1 is greater than +10 kcal mol^{-1}, is thus inconsistent with the observed negative temperature coefficient for ethyl radical oxidation, and is not operative at temperatures below 1000 K.

Finally, we have probed the $\tilde{A}$ ^{2}A′ state of **TS1′**, which corresponds to the $C_2H_5^\bullet$ ($\tilde{X}$ ^{2}A′) + O_2 (a $^1\Delta_g$) reaction. At the

CCSD(T)/TZ2P level using the CCSD(T)/DZP geometry of the ground state, this "vertical" excitation energy is 26.3 kcal mol^{-1}, similar to the 22.3 kcal mol^{-1} a $^1\Delta_g \leftarrow$ X $^3\Sigma_g^-$ excitation energy (T_e) in O_2.[92]

2. Ethylperoxy β-Hydrogen Transfer with O−O Bond Rupture To Yield Oxirane + •OH (M2). The initial step in mechanisms M2 and M4 involves formation of the hydroperoxyethyl radical via β-hydrogen isomerization of the ethylperoxy radical. An understanding of this process is best achieved when one invokes the role of symmetry. Consider the ground ^{2}A″ state of **2**(*trans*). The origin of the a″ SOMO is easily explained by recalling that in O_2 (X $^3\Sigma_g^-$,) there are two unpaired electrons in degenerate π orbitals which are perpendicular to one another about the bond axis. As one of the unpaired electrons in O_2 forms a bond with the a′ radical electron in C_2H_5•, the second unpaired electron remains inactive toward bonding, and thus becomes the "new" radical electron in **2**(*trans*), perpendicular to the plane of reaction.

In the **2**(*cis*-**TS**) (^{2}A″) structure, the terminal oxygen atom is in the proximity of the terminal methyl group, 2.65 Å from C_b at the CCSD(T)/DZP level and ≈1.6 Å from an in-plane hydrogen atom, upon a 60° rotation of the methyl group. The unpaired electron remains perpendicular to the C_s plane of symmetry, which contains the migrating hydrogen (H_b) in the β-hydrogen isomerization process. Likewise, in the lowest energy **2**(*gauche*) conformation, the unpaired electron is directed −75° out of the $O_aO_bH_b''C_b$ "plane", whose framework has a torsion angle of only 6.9°. Clearly, the asymmetric **2**(*gauche*) SOMO retains much of the a″ character of the **2**(*cis*-**TS**) conformer. In the $O_aO_bH_b''C_b$ "plane" the terminal oxygen atom is 2.67 Å from the nearest methyl hydrogen atom, which becomes the migrating hydrogen in the β-hydrogen isomerization process.

Thus, in both the **2**(*cis*-**TS**) and **2**(*gauche*) conformations of the ethylperoxy radical, the unpaired electron is in an a″ or pseudo-a″ orbital with respect to the plane containing the migrating hydrogen. During intramolecular hydrogen transfer, the "radical" electron must shift atomic centers, i.e., move from O_b to C_b, a process which is most easily achieved when the SOMO overlaps with the migrating hydrogen atom, which is not the case in the ground state of either **2**(*cis*-**TS**) or **2**(*gauche*). However, the first excited state of the ethylperoxy radical places the electron in an a′ or pseudo-a′ SOMO and thus in the plane of migration, which facilitates an intramolecular hydrogen transfer.[65,118] A similar situation occurs in the $^{\bullet}CH_3 + O_2$ reaction.[66]

Locating excited states which belong to the C_1 point group is not possible without an equation-of-motion (EOM) formulation of the coupled cluster method, which we have not used. We can, however, study the Ã ^{2}A′ states of the **2**(*trans*) and **2**(*cis*-**TS**) rotamers. Our results for these states are included in Table 4 and pictured in Figure 8. The ^{2}A′ excited surface correlates to C_2H_5• (X̃ ^{2}A′) + O_2 (a $^1\Delta_g$) reactants. Note that the triplet−singlet gap[92] in diatomic O_2 is 22.3 kcal mol^{-1}, which is similar to the 20.4 and 23.9 kcal mol^{-1} X̃−Ã splittings of the trans- and cis-ethylperoxy isomers, respectively. Both the trans and cis excited-state rotamers are true minima and lie 10.1 and 4.3 kcal mol^{-1} below the ground-state reactants, respectively. Thus, in principle, each is energetically accessible during the course of the reaction.

Hence, one scenario for ethylperoxy β-hydrogen transfer would involve the **2**(*cis*-**ES**) structure, which would then allow for hydrogen transfer via a ring-like ^{2}A′ transition state. QGS[67] first located this transition structure (**TS2′**), but reported an a″ frequency of ≈200*i* cm^{-1} which led to a true ^{2}A transition state (**TS2**). Likewise, we have located **TS2′** (see Figure 9). In **TS2′**, the O−O bond lengthens by 0.060 Å and the C−O bond decreases by 0.014 Å over **2**(*cis*-**ES**). Accompanied by decreases of 4.2° and 7.8° in the $O_bO_aC_a$ and $O_aC_aC_b$ angles, respectively, these geometric changes facilitate the hydrogen abstraction process.

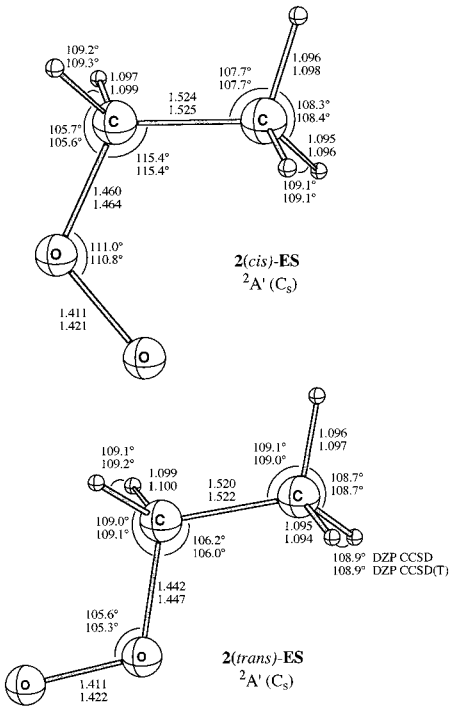

Figure 8. Optimized geometries of the first excited state (Ã ^{2}A′) of the ethylperoxy radical in the cis and trans conformations.

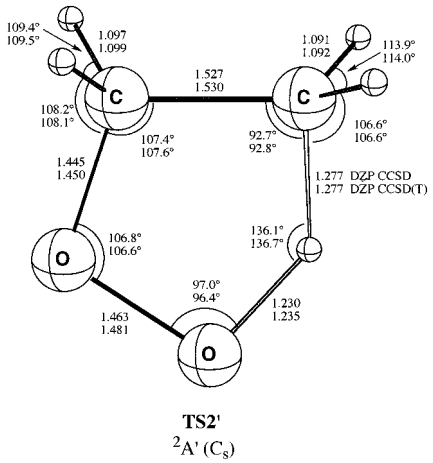

Figure 9. Optimized geometries of the saddle-point structure, **TS2′**, which corresponds to β-hydrogen transfer within the **2**(*cis*-ES) ethylperoxy species.

We also find two imaginary frequencies for **TS2′** of 321*i* (a″) and 2394*i* (a′) cm^{-1}, the former corresponding to ring puckering into the C_1 point group and the latter to intramolecular hydrogen migration. **TS2′** lies 12.2 kcal mol^{-1} above the ground-state reactants and 16.5 above **2**(*cis*-**ES**), representing a relatively small barrier for the actual hydrogen transfer. Yet one must explain why **TS2′** is a saddle point.

To investigate this feature, we performed a CCSD(T)/TZ2P single-point energy computation of the excited ^{2}A″ state of **TS2′** at the ^{2}A′ CCSD(T)/DZP geometry. The optimized ^{2}A″ state would correspond to β-hydrogen transfer from **2**(*cis*-**TS**). Not

surprisingly, due to unfavorable electronic alignment, the **TS2′** $^2A''$ vertical excitation energy is 9.8 kcal mol^{-1}. A second-order Jahn−Teller interaction of the ($^2A'$, $^2A''$) states leads to significant stabilization of asymmetric, C_1 **TS2**. Thus, ethylperoxy radical isomerization to the hydroperoxyethyl radical can proceed through an asymmetric transition state (**TS2**) which is lower in energy than either the $^2A'$ or $^2A''$ states of **TS2′** due to optimal electronic relaxation. We find **TS2** to be 5.1 kcal mol^{-1} lower than **TS2′**, as shown in Figure 1.

Note that **TS2** is actually on the ground-state hypersurface due to the conical intersection of ($^2A'$, $^2A''$) states in C_s configuration space. Indeed, IXAS[74] performed an intrinsic reaction coordinate (IRC) computation which leads backward from **TS2** to the **2**(*gauche*) ethylperoxy radical conformer. This is not entirely unexpected, as the $C_b-C_a-O_a-O_b$ torsion angle in **TS2** is ≈46° with a $C_b-H_b-O_b-O_a$ torsion angle of 15.5°, within reach of the corresponding angles in **2**(*gauche)* of 71.1° and 6.9°; some methyl rotation about the C−C bond yields H_b'' from the migrating hydrogen, H_b.

While QGS[67] were the first to recognize the origin of the asymmetric **TS2** transition state, their results for **TS2** were somewhat dubious due to its abnormally large magnitude of the imaginary frequency. QGS report values of 5981*i* and 4788*i* cm^{-1} at the ROHF/DZP and CISD/DZP levels. However, IXAS[74] found a more reasonable value of 2237*i* cm^{-1} with B3LYP/DZP. We computed frequencies for **TS2** at both the CCSD/DZP and CCSD(T)/DZP levels and find values of 2537*i* and 2637*i* cm^{-1}, respectively. QGS note that the magnitude of imaginary frequencies often correlates with the "sharpness" of a potential barrier. Specifically, in this case, a large energetic barrier correlates with the large imaginary frequencies cited above: E(**TS2**) − E(**2**) in kcal mol^{-1} being 59.7 [ROHF/DZP], 46.4 [CISD/DZP], 41.3 [CCSD/DZP], and 39.1 [CCSD(T)/DZP]. The magnitude of the imaginary frequency appears to level off at about 2600*i* cm^{-1} as the barrier height converges on a value of ≈39 kcal mol^{-1} above **2**.

We have optimized **TS2** (^2A) at levels as sophisticated as CCSD(T)/TZ2P (see Figure 10). At our best level of theory, CCSD(T)/TZ2Pf//CCSD(T)/TZ2P, we find that **TS2** is 5.3 kcal mol^{-1} *above* reactants. The energetics of **TS2** are crucial to deciphering the preferred mechanism of the $C_2H_5^\bullet + O_2$ reaction, and we examine these in our discussion of M4. At this point it is sufficient to realize that the initial barrier in M2 is *above* the ground-state reactants.

The product of the ethylperoxy radical rearrangement via **TS2** is the hydroperoxyethyl radical, **4** (^2A), shown in Figure 11. This radical has a rotamer about the O−O bond, **4′**, which is 0.6 kcal mol^{-1} above **4**. In our geometries of **4** and **4′** the terminal methylene group, $C_bH_b'H_b''$ is twisted about the C−C bond approximately 30° from the B3LYP geometries of IXAS,[74] making the CH_2CH_2 portion of **4** appear more like ethylene. However, the actual orientation of these two hydrogens is of little importance to the overall reaction. We find **4** to be 13.7 kcal mol^{-1} below reactants, or 16.6 kcal mol^{-1} above **2**.

It has long been recognized that **4** can decompose into oxirane + $^\bullet$OH through O−O bond rupture. Our optimized geometries for the decomposition transition state, **TS5** (^2A), are shown in Figure 12. We find that the $C_bC_aO_aO_b$ framework is nearly planar and the O−H hydrogen to be rotated about 50° out of this plane. In a recent study by Chan, Pritchard, and Hamilton,[119] they find a BHLYP/6-311G** geometry quite similar to ours with the exception that the O−H hydrogen is rotated only 6° out of the $C_bC_aO_aO_b$ plane. We obtain an imaginary frequency of 1089*i* cm^{-1} for **TS5**, which is larger than the 655*i* cm^{-1} of Chan et al. To examine **TS5** further we optimized **TS5** at the B3LYP/TZ2Pf level, found the hydroxyl hydrogen to be rotated ≈40° out of the $C_bC_aO_aO_b$ plane, and obtained an imaginary frequency of 745*i* cm^{-1}. Differences between our results and those of Chan et al. are likely due to their use of the BHLYP functional, which incorporates significant Hartree−Fock exchange. IXAS[74] have shown this functional to be less reliable than the B3LYP functional for the $C_2H_5^\bullet + O_2$ reaction.

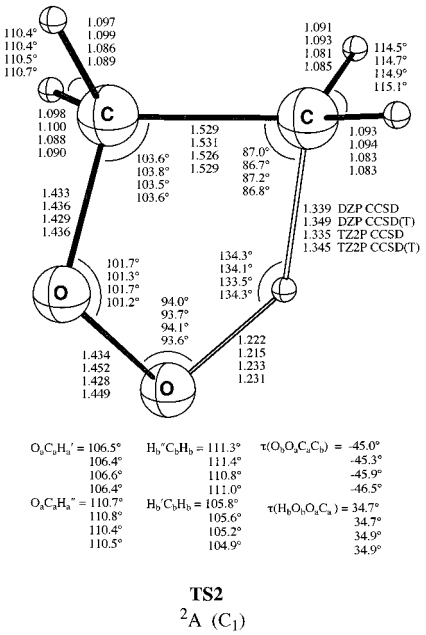

Figure 10. Optimized geometries of the transition state (**TS2**) for the conversion of the ethylperoxy radical (**2**) to the hydroperoxyethyl radical (**4**). See caption of Figure 2 for an explanation of the assumed notation.

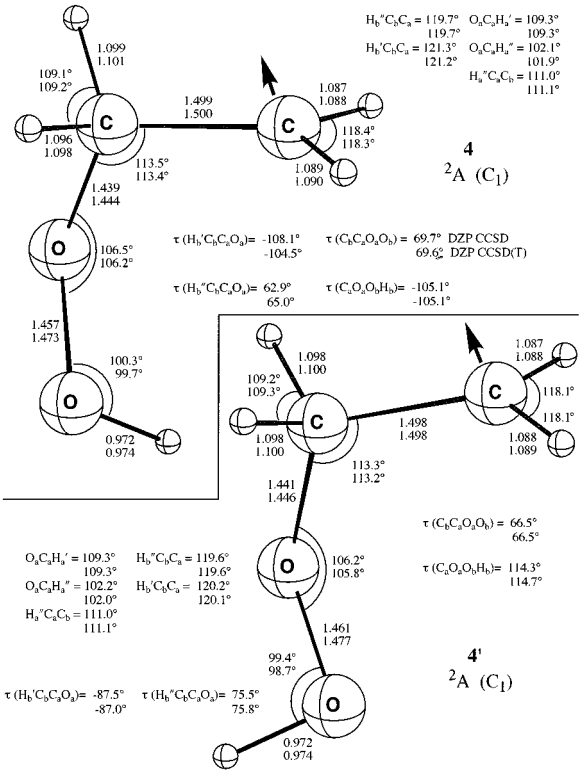

Figure 11. Optimized geometries of the hydroperoxyethyl radical (**4**) and its rotamer (**4′**). See caption of Figure 2 for an explanation of the assumed notation.

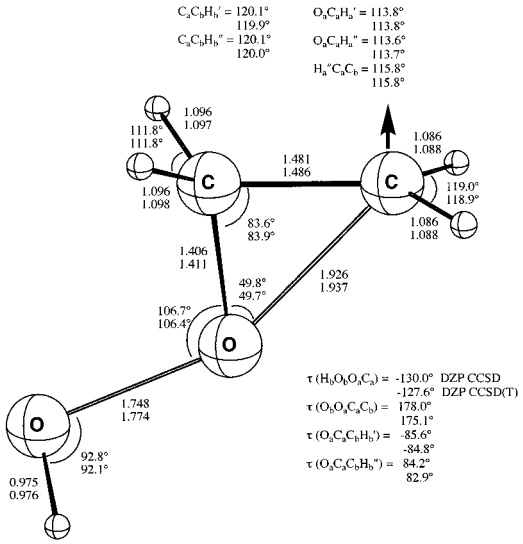

TS5
^2A (C_1)

Figure 12. Optimized geometries of the transition state (**TS5**) for the decomposition of the hydroperoxyethyl radical into oxirane + •OH. See caption of Figure 2 for an explanation of the assumed notation.

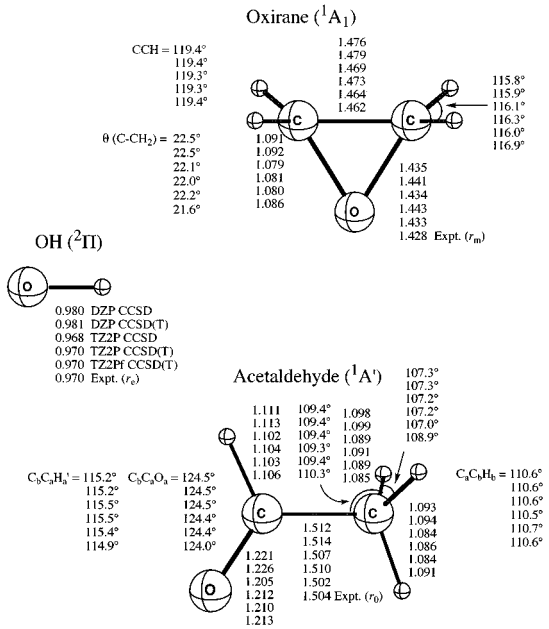

7, 8
Products

Figure 13. Optimized geometries of the products (**7**), oxirane and the hydroxyl radical, and (**8**), acetaldehyde and the hydroxyl radical. The experimental hydroxyl r_e, oxirane r_m and acetaldehyde r_0 values are from refs 92, 127, and 128, respectively. θ(C−CH_2) is an out-of-plane angle.

Chan and co-workers[119] place **TS5** 15.0 kcal mol^{-1} above **4** and 30.6 kcal mol^{-1} above the products, **7**, using UCCSD(T)/6-311G(2d,p) single-point energies at their BHLYP geometries. Earlier density functional studies by Green[85] place **TS5** about 8−9 kcal mol^{-1} above **4** and 14−15 kcal mol^{-1} above products, suggesting a substantially lower barrier. Our RCCSD(T)/TZ2P//RCCSD(T)/DZP values for the same energies are 13.9 and 30.1 kcal mol^{-1}, in good agreement with the values of Chan et al.,[119] as one would anticipate given the similarity in levels of theory.

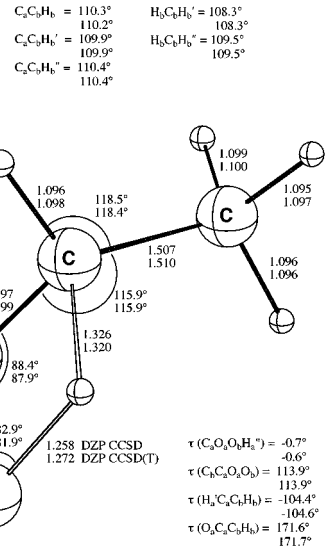

TS4
^2A (C_1)

Figure 14. Optimized geometries of the transition state (**TS4**) for α-hydrogen migration of ethylperoxy radical, **2**. See caption of Figure 2 for an explanation of the assumed notation.

Our best results thus place **TS5** just 0.2 kcal mol^{-1} above C_2H_5• + O_2. Our results are close to the experimental estimate[47] of 16.5 kcal mol^{-1} for the energy of **TS5** relative to **4**, allaying any concerns about the T_1 value of 0.040 for **TS5**. Note in Figure 1 that **TS5** is 5.1 kcal mol^{-1} below **TS2** and hence the overall activation energy for M2 corresponds to **TS2**, for which E_a(0 K) = 5.3 kcal mol^{-1}. Thus it is the initial barrier to hydroperoxyethyl radical formation and not the subsequent decomposition barrier which blocks production of oxirane in the C_2H_5• + O_2 reaction.

3. Ethylperoxy α-Hydrogen Transfer with O−O Bond Rupture To Yield Acetaldehyde + •OH (M3). In contrast to M2 and M4, M3 proceeds through ethylperoxy α-hydrogen transfer. This α-hydrogen transfer is an unfavorable 1,3-suprafacial hydrogen shift. The 1,3-sigmatropic isomerization occurs via a "strained" four-membered ring-like structure, **TS4** (^2A), shown in Figure 14. Note that the $C_a-O_a-O_b-H_a''$ ring is nearly planar. This "strained" species has an imaginary frequency of 2145*i* cm^{-1} and lies, as might be expected, 4.4 kcal mol^{-1} above the corresponding *β*-hydrogen isomerization barrier, **TS2**, and 11.5 kcal mol^{-1} above reactants. M3 has only been examined theoretically in the work of Shen, Moise, and Pritchard,[73] who predicted **TS4** to lie 50.4 kcal mol^{-1} above **2** at the MP4/6-31G//MP2/6-31G level. Our results place **TS4** at 41.8 kcal mol^{-1} above **2**, over 8 kcal mol^{-1} lower than that of Shen et al. and consistent with an expected barrier lowering usually seen with improved correlation treatments.

TS4 leads to formation of the $CH_3\dot{C}HOOH$, **6** (^2A), shown in Figure 15. Shen et al. found **6** to lie 17.2 kcal mol^{-1} above **2**, whereas our results place **6** only 11.9 kcal mol^{-1} above **2**, or 18.4 kcal mol^{-1} below reactants. Shen et al. also found a transition state for dissociation of **6** into products, **TS6** (^2A), which was predicted to lie 8.1 kcal mol^{-1} *below* **6**. No explanation was offered for this apparent anomaly, and we were unable to reproduce their results. It seems likely that the MP2/6-31G method is not capable of correctly describing the bonding in **6** or **TS6**. We have not examined **TS6** but note that the barrier for decomposition into acetaldehyde + •OH, if it exists at all, will probably be small. We also note that the related carbene

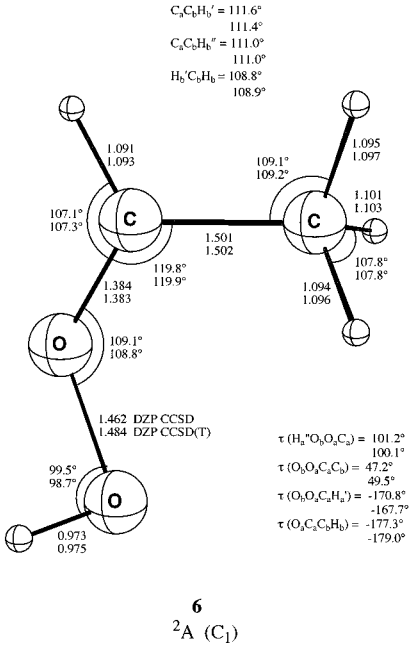

6
^2A (C_1)

Figure 15. Optimized geometries of $CH_3\dot{C}HOOH$ (**6**). See caption of Figure 2 for an explanation of the assumed notation.

species, $CH_3\ddot{C}OOH$, does not appear to have a true O−O bond (≈2.0 Å),[120] whereas **6** has a much shorter peroxy bond of only 1.48 Å at the CCSD(T)/DZP level, quite similar in length to the O−O distance in hydrogen peroxide.[121−123] It is also important to note that the barriers for 1,2-hydrogen migration in either **6** or **4**, which would allow for interconversion between the two species, are likely greater than 40 kcal mol^{-1}.[124]

In summary, although the products of M3, **8**, are the global minimum for the $C_2H_5^\bullet + O_2$ reaction system, the large barrier for α-hydrogen transfer in the ethylperoxy radical of $E_a(0\ K) = 11.5$ kcal mol^{-1} prohibits access to the global minimum at temperatures below 1000 K. We also note that the large activation energy for M3 is consistent with QRRK activation energy estimates[57] of 9.6−10.3 kcal mol^{-1} and experimental observations of virtually no acetaldehyde formation.[41] However, the activation energy for M3 is ≈5 kcal mol^{-1} below the activation energy for M1 and only ≈6 kcal mol^{-1} above that of M2 and M4. Thus M3 should be important at elevated temperatures.

4. Ethylperoxy β-Hydrogen Transfer with C−O Bond Rupture To Yield Ethylene + $HO_2^\bullet$ (M4). As with M2, mechanism M4 proceeds through ethylperoxy β-hydrogen transfer via **TS2**, see Figure 10. In our discussion of M2 we examined symmetry related aspects of this mechanism and noted that with our best level of theory **TS2** lies 5.3 kcal mol^{-1} above reactants. The energy of **TS2** relative to reactants has been the subject of considerable debate. In most experimental work, M4 has been assumed to be the operative mechanism with an activation energy slightly lower than reactants, as indicated by observations of a negative temperature coefficient. From their studies of the $C_2H_5^\bullet + O_2$ reaction, Baldwin, Pickering, and Walker[41] obtained an activation energy of 34.3 ± 2.4 kcal mol^{-1} for β-isomerization of the ethylperoxy radical, which is somewhat less than our value of 37.4 kcal mol^{-1}. In contrast, Slagle, Feng, and Gutman[45] concluded in a subsequent study that **TS2** lies only 23 kcal mol^{-1} above **2** and 6.5 kcal mol^{-1} below reactants, values clearly at odds with our theoretical predictions.

Of particular interest are the RRKM results of Wagner et al.,[58] from which they obtain an overall activation energy for

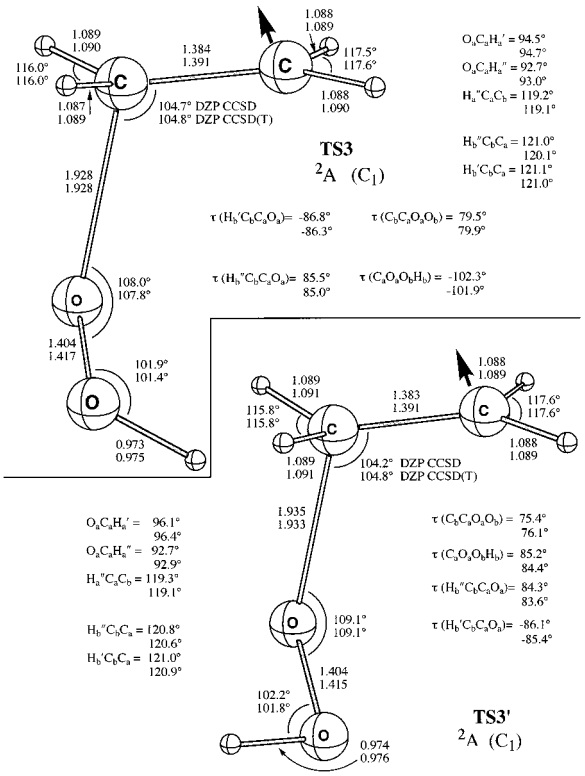

Figure 16. Optimized geometries of the transition state (**TS3**) for the fragmentation of the hydroperoxyethyl radical and its rotamer (**TS3′**). See caption of Figure 2 for an explanation of the assumed notation.

TS2 of −2.4 kcal mol^{-1} (7.7 kcal mol^{-1} lower than our CCSD(T)/TZ2Pf//CCSD(T)/TZ2P value). In hindsight, some parameters used in the RRKM model appear to be erroneous, because ab initio computations of **TS2** were not available at the time of the study, forcing the assignment of approximate geometries and frequencies to **TS2**. For example, our value for the imaginary mode in **TS2** of 2637*i* cm^{-1} is approximately 1000*i* cm^{-1} greater than the 1638*i* cm^{-1} value assumed by Wagner et al. for use in their RRKM modeling. In addition to the assumed imaginary vibrational frequency, Wagner et al. also assume a distance of 1.48 Å for the breaking CH bond. In contrast, our C_bH_b distance in **TS2** is 1.345 Å at the CCSD(T)/TZ2P level of theory. Furthermore, we have already noted that the relative energy of the ethylperoxy radical may be too low in the RRKM studies of Wagner et al. (see section V, part A). These discrepancies and the 7.7 kcal mol^{-1} disagreement between our best computed energy for **TS2** and that of Wagner and co-workers[58] cast doubt on the assumption that the barrier in the RRKM model corresponds to **TS2**, while not necessarily invalidating the value of the barrier height.

TS2 leads to formation of the hydroperoxyethyl radical, **4**. We have already examined **4** in our discussion of M2 and noted that decomposition of **4** into oxirane + $^\bullet$OH proceeded through a barrier of 13.9 kcal mol^{-1}. The hydroperoxyethyl radical can also decompose into ethylene + $HO_2^\bullet$. This fragmentation proceeds through a "loose" transition state, **TS3** (^2A), shown in Figure 16, which is similar in structure to **4**, but with a rather long C···O distance of about 1.9 Å. **TS3** has a rotamer, **TS3′**, which lies 0.9 kcal mol^{-1} above **TS3** and corresponds to decomposition of **4′**. We find **TS3** to lie only 15.1 kcal mol^{-1} above **4** and just 1.4 kcal mol^{-1} above reactants, which is quite similar to the 1.5 kcal mol^{-1} obtained by IXAS.[74] As with **TS1′** and **TS1**, **TS3** leads to the loosely bound $C_2H_4\cdots HO_2^\bullet$ complex, **3**.

The barrier for formation of **4** from the reverse reaction, $C_2H_4 + HO_2^\bullet$ (presumably via **TS3**) has been of much debate. Slagle et al.[45] proposed a barrier height between 5 and 7 kcal mol^{-1} above the products. In contrast, the Arrhenius activation energy obtained by Baldwin, Walker, and co-workers[47,48] placed this barrier at least 17.1 ± 1.2 kcal mol^{-1} above products, a key aspect of their analysis being the assumption that the $C_2H_4 + HO_2^\bullet$ reaction is irreversible. That is, the reaction was assumed to proceed as

$$C_2H_4 + HO_2^\bullet \rightarrow {}^\bullet CH_2CH_2OOH \rightarrow \text{c-}CH_2CH_2O + {}^\bullet OH \quad (10)$$

with the first step being irreversible. In support of this assumption, Baldwin et al.[47,48] argue that decomposition of the hydroperoxyethyl radical, **4**, into oxirane + •OH has a barrier (**TS5**) that is 9.6 kcal mol^{-1} below the barrier for $C_2H_4 + HO_2^\bullet \rightarrow {}^\bullet CH_2CH_2OOH$ (**TS3**). Irreversibility in eq 10 is important as the experiment measured the production of oxirane, and not C_2H_4 or $HO_2^\bullet$ products from reversible processes. Yet subsequent QRRK modeling by Bozzelli and Dean[57] suggested that **TS3** is only 8 kcal mol^{-1} above $C_2H_4 + HO_2^\bullet$.

Using DFT computations, Green[72] placed **TS5** only slightly below (less than 1.5 kcal mol^{-1}) **TS3**. In contrast, Shen, Moise, and Pritchard[73] placed **TS3** 3.3 kcal mol^{-1} below **TS5** with MP4/6-31G//MP2/6-31G theory. Our results place **TS5** below **TS3**, by 1.2 kcal mol^{-1}.

Regardless of the actual ordering of **TS3** and **TS5**, it is clear that both transition states are very close in energy, and should the $C_2H_5^\bullet + O_2$ system overcome the 5.3 kcal mol^{-1} barrier associated with **TS2**, the hydroperoxyethyl radical will likely decompose into both ethylene and oxirane products. Additionally, we find **TS3** to be 14.4 kcal mol^{-1} above $C_2H_4 + HO_2^\bullet$, in large disagreement with the QRRK value of Bozzeili and Dean,[57] and several kcal mol^{-1} lower than values obtained by Baldwin, Walker, and co-workers.[47,48] The close competition between **TS3** and **TS5** clearly vitiates the assumption that eq 10 is irreversible and provides an explanation for apparent, empirical activation energies of Baldwin and co-workers which are too large. We also note that UHF results obtained by Skancke and Skancke[69] suggest that there may exist a transition state leading to oxirane formation directly from $C_2H_4 + HO_2^\bullet$. If such a transition state exists and its relative energy is not much higher than **TS3** and **TS5**, the analysis of the experiments would be further complicated. Clearly there is need for new experimental and theoretical work on the $C_2H_4 + HO_2^\bullet$ reaction.

In summary, M4 is in close competition with M2, and both have the same overall activation energy [$E_a(0\ K) = 5.3$ kcal mol^{-1}]. Additionally, the fact that **TS3** is 1.4 kcal mol^{-1} *above* reactants further argues against M4 as a means for formation of ethylene from the $C_2H_5^\bullet + O_2$ reaction. Because previous experiments below 1000 K have observed very little oxirane formation in the $C_2H_5^\bullet + O_2$ reaction, then M2 is apparently not operative at these temperatures, and because **TS3** and **TS5** are competitive, one must conclude that M4 is also not operative and thus not the primary source of ethylene formation.

5. Concerted Elimination of $HO_2^\bullet$ from the Ethylperoxy Radical To Yield Ethylene + $HO_2^\bullet$ (M5). We have already shown that β-intramolecular hydrogen isomerization in the ground-state ethylperoxy radical is hindered because the orbital of the unpaired electron is not directed in the plane of hydrogen migration. When one considers that the unpaired electron in the products, C_2H_4 (^1A_g) + $HO_2^\bullet$ ($^2A''$), is fully "out-of-plane", it is reasonable to ask whether a simple transition state might connect the ethylperoxy radical directly to products. Indeed, such a transition state was proposed by Baldwin, Dean, and Walker[47] and first studied theoretically by QGS.[67] Our optimized structures for this transition state, **TS1** ($^2A''$), are given in Figure 5. At the CCSD/DZP level an imaginary frequency of 1389*i* cm^{-1} is obtained. It is interesting to note that **TS1** is the cis conformer of the direct hydrogen abstraction transition state, **TS1′**. Indeed, in one sense, **TS1** is itself a direct hydrogen abstraction transition state. However, while IRC computations performed by IXAS[74] for both **TS1′** and **TS1** connect to the loosely bound complex **3** in the forward reaction path, **TS1′** connects to reactants in the reverse reaction path while **TS1** connects to **2**(*gauche*). This is not surprising, as formation of the ethylperoxy radical appears inevitable with nearly every approach of O_2 in the proximity of the $C_2H_5^\bullet$ radical center, because ethylperoxy formation is a barrierless and highly exothermic process.

As with the studies of QGS[67] and IXAS[74] we find **TS1** to be lower in energy than **TS2** and in agreement with IXAS, *below* ground-state reactants. Specifically, at our best level of theory, CCSD(T)/TZ2Pf//CCSD(T)/TZ2P, we find **TS1** to be 6.2 kcal mol^{-1} below **TS2** and 0.9 kcal mol^{-1} below ground-state reactants. IXAS[74] was the first study to find **TS1** *below* reactants. Here, we are the first to confirm this critical result with rigorous, convergent ab initio methods.

We have also examined the first excited state ($^2A'$) of **TS1** at the CCSD(T)/DZP optimized geometry of the ground state ($^2A''$). This vertical excitation energy is 44.2 kcal mol^{-1}, considerably larger than the analogous 9.8 kcal mol^{-1} splitting in **TS2**, and the large state separation prevents significant second-order Jahn−Teller coupling of the two states. Note that both **TS2′** and **TS1** are five-membered ring-like transition states; however, **TS1** displays virtually no C−O bond and a contracted O−O bond, which is shorter than the O−O bond in **TS2′** as well as **TS2**, **2**, and $HO_2^\bullet$. (See Figures 3, 5, 7, and 9.) The electronic ground states of **TS1** and **TS2′** each correspond to the first excited state of the other. Thus, there exists a state crossing, or conical intersection, along the path between the two transition structures.

Our results are of sufficient quality to say with confidence that **TS1** is at or *below* the ground-state reactants, if only by 1 or 2 kcal mol^{-1}. Hence, only M5 has an overall negative activation energy and is compatible with experimental observations of a negative temperature coefficient[45] in the $C_2H_5^\bullet + O_2$ reaction.

Interestingly, our imaginary frequency for **TS1** is only 249*i* cm^{-1} below the 1638*i* cm^{-1} imaginary frequency of **TS2** in the RRKM study of Wagner et al.[58] As already discussed, the model of Wagner et al. could, with structural modification, apply to either M4 or M5, despite the original assumptions of the authors. Certainly, it is equally valid from our perspective to compare our computed barrier heights for either **TS1** or **TS2** with the RRKM barrier height of Wagner et al. Recall that we find a 7.7 kcal mol^{-1} difference between the barrier obtained by Wagner and co-workers and our computed barrier for **TS2**. On the other hand, the RRKM barrier height of −2.4 kcal mol^{-1} is just 1.5 kcal mol^{-1} lower than our barrier for **TS1**. We note again that Wagner et al. may have placed the ethylperoxy radical somewhat too low in energy with respect to reactants. However, the height of **TS1** relative to the ethylperoxy radical from RRKM theory is 30.5 kcal mol^{-1}, a value in excellent agreement with our computed result of 29.4 kcal mol^{-1}. Furthermore, our result of $E_a(0\ K) = -0.9$ kcal mol^{-1} for M5 is in excellent agreement with the recent $C_2H_5^\bullet + O_2$ $E_a(0\ K) = -0.6 \pm 0.1$ kcal mol^{-1} obtained by Dilger et al.[61,62]

C. Comparison to Previous CISD and B3LYP Results. The previous studies from our group, QGS[67,71] and IXAS,[74] were performed with basis sets that are identical or nearly identical to the DZP, TZ2P, and TZ2Pf basis sets used in this study. In Table 6 we compare the results of QGS and IXAS with our present results for three mechanisms: M1, M4, and M5. Of first note, we see that the CCSD(T)/DZP//CISD/DZP values of QGS are all within 1.2 kcal mol^{-1} of our fully optimized CCSD(T)/DZP values. Clearly the results of QGS are quite good. However, while the CCSD(T)/DZP method is often a sufficiently advanced level of theory for many chemical problems, our CCSD(T) results with the TZ2P and TZ2Pf basis are as much as 4.9 kcal mol^{-1} different from their CCSD(T)/DZP counterparts. The B3LYP/TZ2Pf results of IXAS are close to our best values and differ by no more than 3.8 kcal mol^{-1} (excluding **TS1′**).

At all levels of theory, **TS2** remains higher in energy than **TS1**. Examining the convergent ab initio methods [CISD, CCSD, and CCSD(T)], we observe that as the level of theory and basis set increase in sophistication, the relative energy of each transition state decreases with respect to reactants, while the relative energy of **2** and the products, **5**, appear to have already reached convergence at about −30.3 and −12.8 kcal mol^{-1}, respectively. With further improvements in the theoretical treatment, it seems unlikely that the relative energy of each transition state would change by much more than 1 or 2 kcal mol^{-1}, and certainly the energetic ordering of the transition states is even less likely to change. That is, using convergent ab initio techniques, we can say with some confidence that **TS1** is *below* reactants by at least 0.9 kcal mol^{-1}, and is lower in energy than **TS2**, which itself lies *above* reactants by at most 5.3 kcal mol^{-1}.

VI. Conclusions

We have examined five mechanisms for the $C_2H_5^\bullet + O_2$ reaction using high-level ab initio coupled cluster theory. Of mechanisms M1−M5, only M5 is consistent with experimental observations of a negative temperature coefficient. M5 corresponds to concerted elimination of $HO_2^\bullet$ from the ethylperoxy radical gauche conformer, **2**, and has an overall $E_a(0\ K) = -0.9$ kcal mol^{-1}. Our energetics for M4 [$E_a(0\ K) = 5.3$ kcal mol^{-1}] are not consistent with experimental observations of a negative temperature coefficient, and the fact that both **TS2** and **TS3** lie *above* reactants argues against this often assumed mechanism.[45,58] Furthermore, we find that both M2 and M4 will be competitive at higher temperatures, as both have the same activation energy (+5.3 kcal mol^{-1}), and decomposition barriers for the hydroperoxyethyl radical, **4**, into either oxirane (via **TS5**) or ethylene (via **TS3**) are within a 1−2 kcal mol^{-1}. Neither M1, which corresponds to a direct hydrogen abstraction from the ethyl radical by oxygen, nor M3, which leads to formation of acetaldehyde, will be important at temperatures below 1000 K, as both have $E_a(0\ K) > 10$ kcal mol^{-1} relative to reactants.

Several of the most important research groups in the field of combustion chemistry have made important contributions to the $C_2H_5^\bullet + O_2$ problem. Our present results strongly support $C_2H_4 + HO_2^\bullet$ product formation via concerted elimination from the ethylperoxy radical (M5), as originally suggested by Walker and co-workers.[47,49] Wagner, Slagle, Sarzynski, and Gutman[58] have argued against M5 in favor of the two-step mechanism, M4. Wagner et al. reasoned that should M5 exist, "the $HO_2 + C_2H_4$ [reverse] reaction would also proceed along it to a significant extent to form $C_2H_5 + O_2$ instead of exclusively by crossing the high-potential-energy barrier leading to the formation of $CH_2CH_2O_2H$ (followed by the subsequent formation of $C_2H_4O + OH$)". Certainly our results show that each of **TS1**, **TS5**, and **TS3** are competitive (within 1 or 2 kcal mol^{-1}), and thus any interpretation of experimental data for the reverse reaction will be difficult. Without reexamination of the $C_2H_4 + HO_2^\bullet$ reaction, the 1986 study of this reverse reaction by Walker and co-workers[47] should not be exclusively relied upon as evidence against the forward reaction proceeding via M5. In other words, the argument against M5 put forward by Wagner et al.[58] is not conclusive. Indeed, Pilling et al.[65] advocate interpretation of the reverse reaction by considering a composite mechanism, which accounts for formation of the ethylperoxy radical via the concerted mechanism, M5. Since Pilling's review and our studies (QGS[67] and IXS[74]), more recent discussion[20−23,113,118] of the $C_2H_5^\bullet + O_2$ reaction has acknowledged the possibility of M5 as a mechanism for olefin formation. We conclude from this work that this concerted mechanism is the only operative mechanism at low temperatures for the forward reaction.

The concerted elimination mechanism, M5, is distinct from that of the β-hydrogen transfer/elimination mechanism, M4. Indeed, M5 and M4 will have different kinetic implications in terms of the overall ethane oxidation process. For example, the hydroperoxyethyl radical intermediate, **4**, could undergo additional reactions (such as O_2 addition), which would be impossible if the concerted elimination mechanism, M5, is operative, as this mechanism does not involve any geniune intermediates other than the ethylperoxy radical. Furthermore, even if M4 and M5 were to have the same E_a (0 K), the Arrhenius preexponential factors (A factors) would likely noticeably differ. We strongly encourage all large-scale kinetic models of hydrocarbon oxidation to include mechanisms based on both M4 and M5, especially as the latter mechanism has not traditionally been considered.

Finally. we emphasize that the $C_2H_5^\bullet + O_2$ reaction is a prototype reaction for the oxidation of many simple hydrocarbon-based species,[14,15,18,20,50] such as $CH_3\dot{C}HCl$, $C_3H_7^\bullet$, $CH_3\dot{C}Cl_2$, $(CH_3)_2\dot{C}Cl$, and $(CH_3)_3C^\bullet$. Indeed, in a detailed study of the $(CH_3)_3C^\bullet + O_2$ reaction, Chen and Bozzelli[20] found the preferred mechanism proceeded through formation of *tert*-butylperoxy radical with concerted formation of isobutene + $HO_2^\bullet$ through a transition state similar to **TS1**. Furthermore, β-hydrogen isomerization of the *tert*-butylperoxy radical via a **TS2**-like transition state was ≈5 kcal mol^{-1} higher, with barriers to dissociation of the resulting *tert*-butyl hydroperoxide into either isobutene + $HO_2^\bullet$ (via a **TS3**-like transition state) or 2,2-dimethyloxirane + $^\bullet$OH (via a **TS5**-like transition state) being competitive (to within 1 kcal mol^{-1}). Thus, oxidation of the tertiary butyl radical occurs through mechanisms which mirror the surface of the $C_2H_5^\bullet + O_2$ reaction.

Note Added in Proof. Since the completion of this manuscript in early 2000, the ethyl + O_2 reaction has continued to attract research interest from several groups. In an examination of structure−activity relationships in the epoxidation of alkenes by peroxyl radicals, Stark[140] has attempted to reconcile mechanistic conflicts in the observed primary products, specifically, why $C_2H_5^\bullet + O_2$ yields $C_2H_4 + HO_2^\bullet$ whereas $C_2H_4 + HO_2^\bullet$ gives oxirane + $^\bullet$OH. The crux is an extension of the (2A″, 2A′) curve-crossing arguments made here for the interplay of the M2, M4, and M5 (via TS2′, TS2, and TS1) to the exit channel connecting the hydroperoxyethyl radical, **4**, to $C_2H_4 + HO_2^\bullet$ (2A″, 2A′). Chen and Bozzelli[141] have very recently investigated the kinetics and thermochemistry of the addition of $HO_2^\bullet$ to ethylene, propene, and isobutene by means of MP2, MP4, CBS-Q, and B3LYP theory. Finally, preprints sent to us

by Professor Stephen Klippenstein (Case Western Reserve University) and Dr. Craig Taatjes (Sandia National Laboratories, Livermore) also report excellent new theoretical and experimental work for the $C_2H_5^{\bullet} + O_2$ reaction in accord with the overall mechanistic conclusions advanced here. It is clear that forthcoming publications will continue to elevate and even more rigorously analyze this celebrated combustion prototype.

Acknowledgment. This work was supported by the U.S. Department of Energy, Office of Basic Energy Sciences, Division of Chemical Sciences, Fundamental Interactions Branch, Grant No. DOE-DE-FG02-97-ER. J.C.R.K. thanks Professor Daniel Crawford, Professor G. B. Ellison and Dr. E. W. Kaiser for helpful discussions, Christine Rienstra-Kiracofe for research assistance, and Professor P. R. Schreiner for a careful review of the manuscript. We also thank Ed Valeev, Shawn Brown, and Professor Daniel Crawford for implementations within PSI 3.0 which made computation of T_1 diagnostic values possible. The journal cover and Figure 1 artwork were made by Krysia Haag. Finally, we thank Professor Attila Császár, whose visit to the Center for Computational Quantum Chemistry was made possible by a NATO Linkage Grant (CRG.LG 973 892), for helpful discussions and assistance in the early stages of the project.

Supporting Information Available: Two sets of Cartesian coordinates for each species represented in Figures 2−16 corresponding to two levels of theory: CCSD/DZP and the highest level of theory at which the particular species was optimized. Complete quadratic force constants in symmetrized internal coordinates and harmonic vibrational analyses, including the total energy distribution for normal vibrations among the symmetrized internal coordinates. This material is available free of charge via the Internet at http://pubs.acs.org.

References and Notes

(1) Hucknall, D. J. *Chemistry of Hydrocarbon Combustion*; Chapman and Hall: New York, 1985.
(2) Avramenko, L. I.; Kolesnikova, R. V. *Izv. Akad. Nauk, Ser. Khim.* **1960**, *806*, 989.
(3) Barbieri, G.; Di Maio, F. P.; Lignola, P. G. *Combust. Sci. Technol.* **1994**, *98*, 95.
(4) Barbe, P.; Battin-Leclerc, F.; Côme, G. M. *J. Chim. Phys.* **1995**, *92*, 1666.
(5) Hunter, T. B.; Litzinger, T. A.; Wang, H.; Frenklach, M. *Combust. Flame* **1996**, *104*, 505.
(6) Gaffuri, P.; Faravelli, T.; Ranzi, E.; Cernansky, N. P.; Miller, D.; d'Anna, A.; Ciajolo, A. *AIChE J.* **1997**, *43*, 1278.
(7) Hidaka, Y.; Sato, K.; Hoshikawa, H.; Nishimori, T.; Takahashi, R.; Tanaka, H.; Inami, K.; Ito, N. *Combust. Flame* **2000**, *120*, 245.
(8) Lightfoot, P. D.; Cox, R. A.; Crowley, J. N.; Destriau, M.; Hayman, G. D.; Jenkin, M. E.; Moortgat, G. K.; Zabel, F. *Atmos. Environ.* **1992**, *26A*, 1805.
(9) Ghigo, G.; Tonachini, G. *J. Chem. Phys.* **1999**, *110*, 7298.
(10) Frost, G. J.; Ellison, G. B.; Vaida, V. *J. Phys. Chem. A* **1999**, *103*, 10169.
(11) Wallington, T. J.; Dagaut, P.; Kurylo, M. J. *Chem. Rev.* **1992**, *92*, 667.
(12) Bozzelli, J. W.; Dean, A. M. *J. Phys. Chem.* **1993**, *93*, 4427.
(13) Fagerström, K.; Lund, A.; Mahmoud, G.; Jodkowski, J. T.; Ratajczak, E. *Chem. Phys. Lett.* **1993**, *208*, 321.
(14) Knyazev, V. D.; Bencsura, A.; Dubinsky, I. A.; Gutman, D.; Melius, C. F.; Senkan, S. M. *J. Phys. Chem.* **1995**, *99*, 230.
(15) Kaiser, E. W.; Wallington, T. J. *J. Phys. Chem.* **1996**, *100*, 18770.
(16) Atkinson, D. B.; Hudgens, J. W. *J. Phys. Chem. A* **1997**, *101*, 3901.
(17) Tyndall, G. S.; Orlando, J. J.; Wallington, T. J.; Hurley, M. D. *Int. J. Chem. Kinet.* **1997**, *29*, 655.
(18) Kaiser, E. W. *J. Phys. Chem. A* **1998**, *102*, 5903.
(19) Knyazev, V. D.; Bencsura, A.; Slagle, I. R. *J. Phys. Chem. A* **1998**, *102*, 1760.
(20) Chen, C.-J.; Bozzelli, J. W. *J. Phys. Chem. A* **1999**, *103*, 9731.
(21) Loomis, R. A.; Leone, S. R.; Gilles, M. K. *Res. Chem. Intermed.* **1998**, 24, 707.
(22) Venkatesh, P. K.; Dean, A. M.; Cohen, M. H.; Carr, R. W. *J. Chem. Phys.* **1999**, *111*, 8313.
(23) Venkatesh, P. K. *J. Phys. Chem. A* **2000**, *104*, 280.
(24) Bone, W. A. *Nature* **1928**, *122*, 203.
(25) Bone, W. A. *Proc. R. Soc. London, Ser. A* **1932**, *137*, 243.
(26) Semenov, N. *Chemical Kinetics and Chain Reactions*; Oxford: London, 1935.
(27) Cullis, C. F.; Hinshelwood, C. N. *Discuss. Faraday Soc.* **1947**, *2*, 117.
(28) Shuler, K. E. In *5th Symposium (International) on Combustion [Proceedings]*; Reinhold: New York, 1955; p 56.
(29) Knox, J. H.; Norrish, R. G. W. *Trans. Faraday Soc.* **1954**, *50*, 928.
(30) Semenov, N. N. *Some Problems in Chemical Kinetics and Reactivity*; Princeton University Press: Princeton, NJ, 1958; Vol. 1.
(31) Shtern, V. Y. *The Gas-Phase Oxidation of Hydrocarbons*; Pergamon Press Ltd.: New York, 1964.
(32) Lewis, B.; von Elbe, G. *Combustion, Flames, and Explosions of Gases*; Academic Press Inc.: New York, 1961.
(33) Pollard, R. T. *Comprehensive Chemical Kinetics*; Bamford, C. H., Tipper, C. F. H., Eds., Elsevier Scientific: Amsterdam, 1977; Vol. 17, Chapter 2.
(34) Knox, J. H.; Wells, C. H. J. *Trans. Faraday Soc.* **1963**, *59*, 2786.
(35) Knox, J. H.; Wells, C. H. J. *Trans. Faraday Soc.* **1963**, *59*, 2801.
(36) Knox, J. H. *Combust. Flame* **1965**, *9*, 297.
(37) Baker, R. R.; Baldwin, R. R.; Walker, R. W. *J. Chem. Soc., Faraday Trans. 1* **1975**, *71*, 756.
(38) Baldwin, R. R.; Cleugh, C. J.; Walker, R. W. *J. Chem. Soc., Faraday Trans. 1* **1976**, *72*, 1715.
(39) Batt, L.; Robinson, G. N. *Int. J. Chem. Kinet.* **1979**, *11*, 1045.
(40) Baldwin, R. R.; Bennett, J. P.; Walker, R. W. *J. Chem. Soc., Faraday Trans. 1* **1980**, *76*, 1075.
(41) Baldwin, R. R.; Pickering, I. A.; Walker, R. W. *J. Chem. Soc., Faraday Trans. 1* **1980**, *76*, 2374.
(42) Hickel, B. *J. Phys. Chem.* **1975**, *79*, 1054.
(43) Dechaux, J. C.; Delfosse, L. *Combust. Flame* **1979**, *34*, 169.
(44) Fish, A. *Angew. Chem., Int. Ed. Engl.* **1968**, *7*, 45.
(45) Slagle, I. R.; Feng, Q.; Gutman, D. *J. Phys. Chem.* **1984**, *88*, 3648.
(46) Slagle, I. R.; Ratajczak, E.; Gutman, D. *J. Phys. Chem.* **1986**, *90*, 402.
(47) Baldwin, R. R.; Dean, C. E.; Walker, R. W. *J. Chem. Soc., Faraday Trans 2* **1986**, *82*, 1445.
(48) Baldwin, R. R.; Stout, D. R.; Walker, R. W. *J. Chem. Soc., Faraday Trans.* **1991**, *87*, 2147.
(49) McAdam, K. G.; Walker, R. W. *J. Chem. Soc., Faraday Trans. 2* **1987**, *83*, 1509.
(50) Gulati, S. K.; Walker, R. W. *J. Chem. Soc., Faraday Trans. 2* **1988**, *84*, 401.
(51) Plumb, I. C.; Ryan, K. R. *Int. J. Chem. Kinet.* **1981**, *13*, 1011.
(52) Wallington, T. J.; Andino, J. M.; Kaiser, E. W.; Japar, S. M. *Int. J. Chem. Kinet.* **1989**, *21*. 1113.
(53) Kaiser, E. W.; Rimai, L.; Wallington, T. J. *J. Phys. Chem.* **1989**, *93*, 4094.
(54) Kaiser, E. W.; Lorkovic, I. M.; Wallington, T. J. *J. Phys. Chem.* **1990**, *94*, 3352.
(55) Kaiser, E. W.; Wallington, T. J.; Andino, J. M. *Chem. Phys. Lett.* **1990**, *168*, 309.
(56) Niki, H.; Maker, P. D.; Savage, C. M.; Breitenbach, L. P. *J. Phys. Chem.* **1982**, *86*, 3825.
(57) Bozzelli, J. W.; Dean, A. M. *J. Phys. Chem.* **1990**, *94*, 3313.
(58) Wagner, A. F.; Slagle, I. R.; Sarzynski, D.; Gutman, D. *J. Phys. Chem.* **1990**, *94*, 1853.
(59) Dobis, O.; Benson, S. W. *J. Am. Chem. Soc.* **1993**, *115*, 8798.
(60) Fenter, F. F.; Catoire, V.; Lesclaux, R.; Lightfoot, P. D. *J. Phys. Chem.* **1993**, *97*, 3530.
(61) Dilger, H.; Schwager, M.; Tregenna-Piggott, P. L. W.; Roduner, E.; Reid, I. D.; Arseneau, D. J.; Pan, J. J.; Senba, M.; Shelley, M.; Fleming, D. G. *J. Phys. Chem.* **1996**, *100*, 6561.
(62) Dilger, H.; Schwager, M.; Tregenna-Piggott, P. L. W.; Roduner, E.; Reid, I. D.; Arseneau, D. J.; Pan, J. J.; Senba, M.; Shelley, M.; Fleming, D. G. *J. Phys. Chem.* **1996**, *100*, 16445.
(63) Kaiser, E. W. *J. Phys. Chem.* **1995**, *99*, 707.
(64) Walker, R. W. In *Major Research Topics in Combustion*; Hussaini, M. Y., Kumar, A., Voigt, R. G., Eds.; Springer-Verlag: New York, 1992; p 277.
(65) Pilling, M. J.; Robertson, S. H.; Seakins, P. W. *J. Chem. Soc., Faraday Trans.* **1995**, *91*, 4179.
(66) Walch, S. P. *Chem. Phys. Lett.* **1993**, *215*, 81.
(67) Quelch, G. E.; Gallo, M. M.; Shen, M.; Xie, Y.; Schaefer, H. F.; Moncrieff, D. *J. Am. Chem. Soc.* **1994**, *116*, 4953.
(68) Dilger, H.; Schwager, M.; Roduner, E.; Reid, I. D.; Fleming, D. G. *Hyperfine Interact.* **1994**, *87*, 899.
(69) Skancke, A.; Skancke, P. N. *J. Mol. Struct. (THEOCHEM)* **1990**, *207*, 201.

(70) Boyd, S. L.; Boyd, R. J.; Barclay, L. R. C. *J. Am. Chem. Soc.* **1990**, *112*, 5724.
(71) Quelch, G. E.; Gallo, M. M.; Schaefer, H. F. *J. Am. Chem. Soc.* **1992**, *114*, 8239.
(72) Green, W. H. *Int. J. Quantum Chem.* **1994**, *52*, 837.
(73) Shen, D.; Moise, A.; Pritchard, H. O. *J. Chem. Soc., Faraday Trans.* **1995**, *91*, 1425.
(74) Ignatyev, I. S.; Xie, Y.; Allen, W. D.; Schaefer, H. F. *J. Chem. Phys.* **1997**, *107*, 141.
(75) Purvis, G. D.; Bartlett, R, J. *J. Chem. Phys.* **1982**, *76*, 1910.
(76) Rittby, M.; Bartlett, R. J. *J. Phys. Chem.* **1988**, *92*, 3033.
(77) Raghavachari, K.; Trucks, G. W.; Pople, J. A.; Head-Gordon, M. *Chem. Phys. Lett.* **1989**, *157*, 479.
(78) Bartlett, R. J.; Watts, J. D.; Kucharski, S. A.; Noga, J. *Chem. Phys. Lett.* **1990**, *165*, 513.
(79) Bartlett, R. J.; Watts, J. D.; Kucharski, S. A.; Noga, J. *Chem. Phys. Lett.* **1990**, *167*, 609.
(80) Gauss, J.; Lauderdale, W. J.; Stanton, J. F.; Watts, J. D.; Bartlett, R. J. *Chem. Phys. Lett.* **1991**, *182*, 207.
(81) ACES II is a program product of the Quantum Theory Project, University of Florida. Authors: J. F. Stanton, J. Gauss, J. D. Watts, M. Nooijen, N. Oliphant, S. A. Perera, P. G. Szalay, W. J. Lauderdale, S. R. Gwaltney, S. Beck, A. Balkova, D. E. Bernholdt, K.-K. Baeck, P. Rozyczko, H. Sekino, C. Hober, and R. J. Bartlett. Integral packages included are VMOL (J. Almlöf and P. R. Taylor); VPROPS (P. Taylor); ABACUS (T. Helgaker, H. J. Aa. Jensen, P. Jorgensen, J. Olsen, and P. R. Taylor).
(82) Huzinaga, S. *J. Chem. Phys.* **1965**, *42*, 1293.
(83) Dunning, T. H., Jr. *J. Chem. Phys.* **1970**, *53*, 2823.
(84) Dunning, T. H., Jr. *J. Chem. Phys.* **1971**, *55*, 716.
(85) Frisch, M. J.; Trucks, G. W.; Schlegel, H. B.; Gill, P. M. W.; Johnson, B. G.; Robb, M. A.; Cheeseman, J. R.; Keith, T.; Petersson, G. A.; Montgomery, J. A.; Raghavachari, K.; Al-Laham, M. A.; Zakrzewski, V. G.; Ortiz, J. V.; Foresman, J. B.; Cioslowski, J.; Stefanov, B. B.; Nanayakkara, A.; Challacombe, M.; Peng, C. Y.; Ayala, P. Y.; Chen, W.; Wong, M. W.; Andres, J. L.; Replogle, E. S.; Gomperts, R.; Martin, R. L.; Fox, D. J.; Binkley, J. S.; Defrees, D. J.; Baker, J.; Stewart, J. P.; Head-Gordon, M.; Gonzalez, C.; Pople, J. A. *Gaussian 94* (Revision C.3), Gaussian, Inc.: Pittsburgh, PA, 1995.
(86) Jayatilaka, D.; Lee, T. J. *J. Chem. Phys.* **1993**, *98*, 9734.
(87) Crawford, T. Daniel; Sherrill, C. David; Valeev, Edward F.; Fermann, Justin T.; Leininger, Matthew L.; King, Rollin A.; Brown, Shawn T.; Janssen, Curtis L.; Seidl, Edward T.; Yamaguchi, Yukio; Allen, Wesley D.; Xie, Yaoming; Vacek, George; Hamilton, Tracy P.; Kellogg, C. Brian; Remington, Richard B.; Schaefer, Henry F., III. PSI 3.0 development version, PSITECH, Inc., Watkinsville, GA 30677, 1999.
(88) Martin, J. M. L.; Taylor, P. R. *Chem. Phys. Lett.* **1996**, *248*, 336.
(89) Wong, M. W.; Baker, J.; Nobes, R. H.; Radom, L. *J. Am. Chem. Soc.* **1987**, *109*, 2245.
(90) Davis, S.; Uy, D.; Nesbitt, D. J. *J. Chem. Phys.* **2000**, *112*, 1823.
(91) Duncan, J. L.; McKean, D. C.; Mallinson, P. D. *J. Mol. Spectrosc.* **1973**, *45*, 221.
(92) Huber, K. P.; Herzberg, G. *Molecular Spectra and Molecular Structure. IV. Constants of Diatomic Molecules;* Van Nostrand Reinhold: New York, 1979.
(93) Lee, T. J.; Allen, W. D.; Schaefer, H. F. *J. Chem. Phys.* **1987**, *87*, 7062.
(94) Ahern, A. M.; Garrell, R. L.; Jordan, K. D. *J. Phys. Chem.* **1988**, *92*, 6228.
(95) Martin, J. M. L.; Lee, T. J.; Taylor, P. R.; François, J. P. *J. Chem. Phys.* **1995**, *103*, 2589.
(96) Shimanouchi, T. *Tables of Molecular Vibrational Frequencies Consolidated Volume I*; National Bureau of Standards: Washington, DC, 1972.
(97) Pacansky, J.; Dupuis, M. *J. Am. Chem. Soc.* **1982**, *104*, 415.
(98) Chettur, G.; Snelson, A. *J. Phys. Chem.* **1987**, *91*, 3483.
(99) Pacansky, J.; Koch, W.; Miller, M. D. *J. Am. Chem. Soc.* **1991**, *113*, 317.
(100) Uehara, H.; Kawaguchi, K.; Hirota, E. *J. Chem. Phys.* **1985**, *83*, 5479.
(101) For the ethylperoxy radical we compared the **2**(*gauche*) harmonic frequencies to the experimental values, as harmonic frequencies for the three other rotamers are quite similar. See ref 74 and supporting information for this paper.
(102) Grev, R. S.; Janssen, C. L.; Schaefer, H. F. *J. Chem. Phys.* **1991**, *95*, 5128.
(103) Lee, T. J.; Rice, J. E.; Scuseria, G. E.; Schaefer, H. F. *Theor. Chim. Acta* **1989**, *75*, 81.
(104) Lee, T. J.; Taylor, P. R. *Int. J. Quantum Chem.* **1989**, *23*, 199.
(105) Watts, J. D.; Gauss, J.; Bartlett, R. J. *Chem. Phys. Lett.* **1992**, *200*, 1.
(106) Lauderdale, W. J.; Cheng, V. G.; Wierschke, S. G. *J. Phys. Chem.* **1994**, *98*, 4502.
(107) Murray, C. W.; Handy, N. C. *J. Chem. Phys.* **1992**, *97*, 6509.
(108) Lauderdale, W. J.; Stanton, J. F.; Gauss, J.; Watts, J. D.; Bartlett, R. J. *Chem. Phys. Lett.* **1991**, *187*, 21.
(109) Lauderdale, W. J.; Stanton, J. F.; Gauss, J.; Watts, J. D.; Bartlett, R. J. *J. Chem. Phys.* **1992**, *97*, 6606.
(110) Urban, M.; Watts, J. D.; Bartlett, R. J. *Int. J. Quantum Chem.* **1994**, *52*, 211.
(111) In organic stereochemical notation the rotamers: **2**(*gauche*), **2**(*gauche*-**TS**), **2**(*trans*), and **2**(*cis*-**TS**) are denoted as the syn-clinal, anti-clinal, anti-periplanar, and syn-periplanar conformations of the ethylperoxy radcial about the C−O bond. See: Eliel, E. L. *Elements of Stereochemistry*; John Wiley & Sons: New York, 1969; p 25.
(112) Benson, S. W. *J. Phys. Chem.* **1996**, *100*, 13544.
(113) Knyazev,V. D.; Slagle, I. R. *J. Phys. Chem. A* **1998**, *102*, 1770.
(114) Brinck,T.; Lee, H. N.; Jonsson, M. *J. Phys. Chem. A* **1999**, *103*, 7094.
(115) Benson, S. W.; Cohen, N. In *Peroxyl Radicals;* Alfassi, Z. B., Ed.; John Wiley and Sons: Chichester, UK, 1997; p 49.
(116) Benson, S. W. *J. Am. Chem. Soc.* **1965**, *87*, 972.
(117) Harding, L. B.; Wagner, A. F. *J. Phys. Chem.* **1986**, *90*, 2974.
(118) Clifford, E. P.; Wenthold, P. G.; Gareyev, R.; Lineberger, W. C.; Depuy, C. H.; Bierbaum, V. M.; Ellison, G. B. *J. Chem. Phys.* **1998**, *109*, 10293.
(119) Chan, W. T.; Pritchard, H. O.; Hamilton, I. P. *Phys. Chem. Chem. Phys.* **1999**, *1*, 3715.
(120) Richardson, N. A.; Rienstra-Kiracofe, J. C.; Schaefer, H. F. *J. Am. Chem. Soc.* **1999**, *121*, 10813.
(121) Giguere, P. A.; Srinivasan, T. K. K. *J. Mol. Spectrosc.* **1977**, *66*, 168.
(122) Cremer, D.; Christen, D. J. *J. Mol. Spectrosc.* **1979**, *74*, 480.
(123) Koput, J. *J. Mol. Spectrosc.* **1986**, *115*, 438.
(124) Harding, L. *J. Am. Chem. Soc.* **1981**, *103*, 7469.
(125) Duncan, J. L.; Wright, I. J.; Van Lerberghe, D. *J. Mol. Spectrosc.* **1972**, *42*, 463.
(126) Lubic, K. G.; Amano, T.; Uehara, H.; Kawaguchi, K.; Hirota, E. *J. Chem. Phys.* **1984**, *81*, 4826.
(127) Hirose, C. *Bull. Chem. Soc. Jpn.* **1974**, *47*, 1311.
(128) Harmony, M. D.; Laurie, V. W.; Kuczkowski, R. L.; Schwendeman, R. H.; Ramsay, D. A.;Lovas, F. J.; Lafferty, W. J.; Maki, A. G. *J. Phys. Chem. Ref. Data* **1979**, *8*, 619.
(129) Berkowitz, J.; Ellison, G. B.; Gutman, D. *J. Phys. Chem.* **1994**, *98*, 2744.
(130) Chase, M. W., Jr. *J. Phys. Chem. Ref. Data* **1998**, Monograph No. 9.
(131) Pedley, J. B.; Naylor, R. D.; Kirby, S. P. *Thermochemical Data of Organic Compounds*; Chapman and Hall: New York, 1986.
(132) Marshall, P. *J. Phys. Chem. A* **1999**, *103*, 4560.
(133) East, A. L. L.; Bunker, P. R. *Chem. Phys. Lett.* **1998**, *282*, 49.
(134) Sears, T. J.; Johnson, P. M.; BeeBe−Wang, J. *J. Chem. Phys.* **1999**, *111*, 9213.
(135) Johnson, P. M.; Sears, T. J. *J. Chem. Phys.* **1999**, *111*, 9222.
(136) Pitzer, K. S.; Gwinn, W. D. *J. Chem. Phys.* **1942**, *10*, 428.
(137) Janz, G. J. *Thermodynamic Properties of Organic Compounds*; Academic Press: New York, 1967.
(138) Belov, S. P.; Tretyakov, M. Y.; Kleiner, I.; Hougen, J. T. *J. Mol. Spectrosc.* **1993**, *160*, 61.
(139) Gu, H.; Kundu, T.; Goodman, L. *J. Phys. Chem.* **1993**, *97*, 7194.
(140) Stark, M. S. *J. Am. Chem. Soc.* **2000**, *122*, 4162.
(141) Chen, C.-J.; Bozzelli, J. W. *J. Phys. Chem. A* **2000**, *104*, 4997.